Electronic Supplementary Material (ESI) for ChemComm.

Supporting Information

Multielectron C–H Photoactivation with an Sb(V) Oxo Corrole

Christopher M. Lemon, Andrew G. Maher, Anthony R. Mazzotti,
David C. Powers, Miguel I. Gonzalez, and Daniel G. Nocera*

Department of Chemistry and Chemical Biology, Harvard University, 12 Oxford Street, Cambridge, MA 02138

dnocera@fas.harvard.edu

Index *Page*

Materials S4
Synthetic details S4
Physical measurements S5
Femtosecond and nanosecond laser details S6
Computational details S7
X-ray crystallographic details S8
NMR spectral details S9
NMR spectra S10
Figure S1. Cyclic voltammograms and spectroelectrochemistry of **2** S13
Figure S2. Ultrafast fluorescence decay trace of **2** S14
Figure S3. Nanosecond transient absorption (TA) spectrum of **2** S15
Figure S4. DFT-optimized geometry of **2** monomer S16
Figure S5. DFT-optimized geometry of **2** S17
Figure S6. Frontier molecular orbitals of **2** monomer S18
Figure S7. Four highest occupied molecular orbitals of **2** S19
Figure S8. Four lowest unoccupied molecular orbitals of **2** S20
Figure S9. Simulated UV-vis spectrum of **2** monomer S21
Figure S10. Primary orbital transition associated with S_5 of **2** monomer S22
Figure S11. Orbitals of **2** monomer and **2** with Sb–O antibonding character S23
Figure S12. Photolysis of **2** in the presence of 1,3-cyclohexadiene S24
Figure S13. Photolysis of **2** in benzene S25
Figure S14. Photolysis of **2** in tetrahydrofuran S26
Figure S15. Photolysis of **2** in acetonitrile S27
Figure S16. Photolysis of **2** in 2-propanol S28
Figure S17. Photolysis of **2** in cycloheptane S29
Figure S18. Comparison of photolysis of **2** in toluene versus toluene-d_8 S30
Figure S19. Photolysis of **2** in toluene-d_8 S31
Figure S20. Conversion of **2** to **1** in toluene and toluene-d_8 as a function of time S32
Figure S21. GC-MS analysis of the photoproducts from photolysis of **2** in toluene S33
Table S1. Summary of crystallographic data S34
Table S2. Cartesian coordinates for the optimized geometry of **2** monomer S35
Table S3. Cartesian coordinates for the optimized geometry of **2** S37
Table S4. TD-DFT calculated singlets for **2** monomer S41
Table S5. TD-DFT calculated triplets for **2** monomer S42
References S43

Materials

The following materials were used as received: hexanes, dichloromethane (CH_2Cl_2), toluene, 1,3-cyclohexadiene, cycloheptane, acetonitrile (MeCN), ethanol (EtOH), benzene, inhibitor-free tetrahydrofuran (THF), 2-propanol, benzonitrile, benzaldehyde, benzyl alcohol, ^{18}O water (97 atom %), urea hydrogen peroxide (H_2O_2•urea), iodosobenzene diacetate ($PhI(OAc)_2$), Nile blue, and silica gel 60 Å 230–400 mesh (40–63 μm particle size) from Sigma-Aldrich; chloroform-*d* ($CDCl_3$) and toluene-d_8 from Cambridge Isotope Laboratories; and iodosobenzene (PhIO) from TCI. Tetrabutylammonium hexafluorophosphate ([TBA][PF_6]) from Sigma-Aldrich was recrystallized from EtOH and subsequently dried under vacuum prior to use. Acetonitrile (MeCN) for electrochemical experiments was obtained from a solvent drying system (Pure Process Technologies) and stored over 3 Å molecular sieves. The Sb(III) complex of 10-(4-methoxycarbonylphenyl)-5,15-bis(pentafluorophenyl)corrole (**1**) was prepared according to literature methods.[1]

Synthesis of 10-(4-methoxycarbonylphenyl)-5,15-bis(pentafluorophenyl)corroloto-(oxo) antimony(V) dimer (2)

Method 1. In a 50 mL round bottom flask, 16 mg (18 μmol) of the Sb(III) complex of 10-(4-methoxycarbonylphenyl)-5,15-bis(pentafluorophenyl) corrole (**1**)[1] was dissolved in 10 mL of MeCN and 23 mg of H_2O_2•urea (240 μmol) was added. The green solution was sonicated for approximately 1 min to solubilize the urea hydrogen peroxide. The reaction mixture was stirred overnight at room temperature, while protected from ambient light. Over the course of the reaction, the solution turned dark red with a violet hue. Solvent was removed by rotary evaporation, and the residue was collected and then re-dissolved in a minimal amount of CH_2Cl_2 and filtered over a small plug of silica using CH_2Cl_2 as the eluent; the desired product eluted as a red-purple solution. After solvent removal, 12 mg (74% yield) of the title compound was isolated as a red-purple solid.

Method 2. In a scintillation vial, 28 mg of **1** (32 μmol) was dissolved in 5 mL of CH_2Cl_2 and 32 mg of $PhI(OAc)_2$ (99 μmol) was added. The resultant solution was stirred at room temperature for 1 h. The crude reaction mixture was filtered over a plug of silica gel using CH_2Cl_2 as the eluent. To remove the iodobenzene, the compound was purified on a silica gel column using CH_2Cl_2 as the eluent. The desired product eluted as a red solution, affording 17 mg (56 % yield) of the title compound.

Method 3. In a scintillation vial, 11 mg of **1** (13 μmol) was dissolved in 4 mL of CH_2Cl_2 and 9 mg of PhIO (41 μmol) was added. The resultant solution was stirred at room temperature for 5 min. The crude reaction mixture was filtered over a plug of silica gel, first using hexane to remove the iodobenzene, then CH_2Cl_2 to elute the desired product. Solvent was removed to give 8 mg (71 % yield) of the title compound.

^{1}H NMR (500 MHz, $CDCl_3$, 25 °C) δ 4.20 (s, 6H), 7.55 (d, *J* = 7.9 Hz, 2H), 7.89 (d, *J* = 7.9 Hz, 2H), 8.36 (d, *J* = 4.2 Hz, 4H), 8.38 (d, *J* = 7.9 Hz, 2H), 8.40 (d, *J* = 4.7 Hz, 4H), 8.44 (d, *J* = 7.8 Hz, 2H), 8.51 (d, *J* = 4.8 Hz, 4H), 8.80 (d, *J* = 4.2 Hz, 4H). ^{19}F NMR (470 MHz, $CDCl_3$, 25 °C) δ –164.63 (m, 4F), –163.11 (m, 4F), –154.11 (t, *J* = 20.8 Hz, 4F), –139.31 (dd, J^1 = 24.3 Hz, J^2 = 7.4 Hz, 4F), –137.58 (d, *J* = 22.8 Hz, 4F). ^{13}C NMR (100 MHz, $CDCl_3$, 25 °C) δ 52.69, 116.89, 121.54, 125.04, 125.62, 126.30, 127.73, 127.84, 128.04, 128.17, 129.18, 131.50, 132.29, 132.75, 134.87, 136.38, 136.86, 139.26, 141.39, 167.18. Anal. Calcd. for $(2M + H)^+$ and $(M + H)^+$, M = $C_{39}H_{15}F_{10}N_4O_3Sb$: 1797.0123 and 899.0101; Found ESI-MS: 1797.0118 and 899.0067. Uv-vis (toluene), λ in nm (ε in 10^3 M^{-1} cm^{-1}): 411 (242), 510 (5.4), 538 (11), 577 (22), 599 (30). Emission (toluene, λ_{ex} = 410 nm), λ in nm: 610, 661.

Physical Measurements

NMR spectra were recorded on a Varian Inova-500 or JEOL ECZ400S NMR spectrometer at the Harvard University Department of Chemistry and Chemical Biology Laukien-Purcell Instrumentation Centre. ^{1}H and ^{13}C NMR spectra were internally referenced to the residual solvent signal (δ = 7.26 (^{1}H) or 77.16 (^{13}C) for $CHCl_3$ in $CDCl_3$),[2] while ^{19}F NMR spectra were externally referenced to α,α,α-trifluorotoluene (δ = –63.72). Mass spectra were recorded on an Agilent 6210 TOF LC/MS mass spectrometer in positive ion mode at the Small Molecule Mass Spectrometry Facility, part of the Harvard FAS Centre for Systems Biology. Gas chromatography–mass spectrometry (GC-MS) analysis was performed using a Shimadzu GC-2010 equipped with a Restek 30 m Rxi-5ms fused silica capillary column interfaced to a Shimadzu QP2010X mass spectrometer via a temperature-programmable transfer line. Helium was used as the carrier gas at a pressure of 150 kPa, giving a linear velocity of 58.9 cm/s. Both the injection port and transfer line were operated at 250 °C. The column was held at 50 °C for 3 min, then increased by 60 °C/min to a final temperature of 250 °C, which was then held for 3.67 min. Calibration curves were generated using authentic samples of benzaldehyde and benzyl alcohol; all samples were spiked with benzonitrile as an internal standard. UV–vis absorption spectra were acquired using a Cary 5000 spectrometer (Agilent) or CCD array spectrophotometer (SI Photonics, Inc). Steady-state emission spectra were recorded on a Photon Technology International (PTI) QM4 fluorometer equipped with a 150 W Xe arc lamp and a Hamamatsu R2658 photomultiplier tube. The relative quantum yield of the Sb corrole in toluene (η = 1.4961)[3] was calculated using Nile blue in EtOH (η = 1.3611)[3] as the reference (Φ_{ref} = 0.27)[4] according to the following equation:

$$\Phi_{sam} = \Phi_{ref}\left(\frac{\nabla_{sam}}{\nabla_{ref}}\right)\left(\frac{\eta_{sam}}{\eta_{ref}}\right)^2 \quad (1)$$

where ∇ is the slope of the plot of integrated fluorescence intensity versus absorbance (constructed with 5 points) and η is the refractive index of the solvent. Air-free corrole samples for transient absorption spectra, triplet lifetimes, and photolysis experiments were prepared using three cycles of freeze–pump–thaw (FPT) to pressures below 10^{-5} Torr. Steady-state photochemical reactions were performed using a 1000 W high-pressure Hg/Xe arc lamp (Oriel). The beam was passed through a water-jacketed filter holder containing a 305 nm long pass filter then through an iris and collimating lens before entering the sample, which was in a quartz cuvette placed in a water-jacketed sample holder to maintain a constant temperature. Electrochemical measurements were made in a glovebox under a nitrogen atmosphere using a CH instruments Electrochemical Workstation using CHI Version 10.03 software. Samples were prepared at concentrations of ~1 mM with 0.1 M [TBA][PF_6] as the supporting electrolyte in acetonitrile. Cyclic voltammograms (CVs) were recorded at a scan rate of 100 mV/s using a glassy carbon button working electrode, a Ag wire reference electrode, and a Pt wire counter electrode. The CVs were internally referenced to ferrocene. Thin-layer UV-vis spectroelectrochemistry experiments were performed using a 0.5 mm path length quartz cell with an Ocean Optics USB4000 spectrophotometer and DT-Mini-2GS UV-vis-NIR light source in conjunction with the CH electrochemical workstation described above. Samples were prepared at concentrations of ~0.2 mM with 0.1 M [TBA][PF_6] in acetonitrile. Bulk electrolysis was performed using a Pt flag working electrode, a Ag wire reference electrode, and a Pt wire counter electrode.

Femtosecond and Nanosecond Laser Details

Picosecond-resolved emission lifetime measurements were acquired using a Libra-F-HE (Coherent) chirped–pulse amplified Ti:sapphire laser system that has been previously described.[5] The 800 nm laser output was used to pump an OPerA Solo (Coherent) optical parametric amplifier (OPA); excitation pulses of 400 nm were produced via fourth harmonic generation of the pump beam using a BBO crystal and the pulse power was attenuated to 2–3 mW at the sample using neutral density filters. Emission lifetimes were measured on a Hamamatsu C4334 Streak Scope streak camera, which has been described elsewhere.[6] The emission signal was collected over a 140 nm window centered at 630 nm with a 1 ns time window using a Stanford Research Systems DG535 delay generator.

Nanosecond transient absorption (TA) spectra were acquired using a previously reported system.[7,8] Pump light was provided by the third harmonic (355 nm) of a Quanta-Ray Lab-190 Nd:YAG laser (Spectra Physics) operating at 10 Hz. The pump light was passed through a BBO crystal in an optical parametric oscillator (OPO), yielding a visible frequency that was tuned to 600 nm. Excitation light was attenuated to 0.5–2.0 mJ per pulse for all experiments using neutral density filters. Probe white light was generated using a 75 W Xe arc lamp (PTI). The probe beam was aligned with the sample while the laser pump beam was positioned at 15° with respect to the white light probe and both beams were focused

on the sample. After exiting the sample, the light entered a iHR320 monochromator (Horiba Scientific) and was dispersed by a blazed grating (500 nm, 300 grooves/mm) centered at 450 nm. The entrance and exit slits of the monochromator were set to provide a spectral resolution of 2 nm. TA spectra were collected using a gated intensified CCD camera (DH520-25F-01, Andor Technology). Acquisition delays and gate times for the CCD were set using a Stanford Research Systems DG535 delay generator, which was synchronized to the Q-switch output of the laser. The final data were calculated from a combination of four spectra: I (pump on/probe on), I_F (pump on/probe off), I_0 (pump off/probe on), and I_B (pump off/probe off). The resultant TA spectra were obtained using the following equation:

$$\Delta\mathrm{OD} = -\log\left(\frac{I-I_F}{I_0-I_B}\right) \quad (2)$$

thereby correcting for both sample emission and extraneous background light. In order to acquire these four spectra, pump and probe beams were selectively exposed to the sample using electronically controlled shutters (Uniblitz T132, Vincent Associates), which were triggered using a Stanford Research Systems DG535 delay generator synchronized to the Q-switch output of the laser. For single wavelength kinetics measurements, output signal from the sample was amplified by a photomultiplier tube (R928, Hamamatsu) and collected on a 1 GHz digital oscilloscope (9384CM, LeCroy); acquisition was triggered using a photodiode to collect scattered laser excitation light.

Computational Details

Density functional theory (DFT) calculations were performed with the hybrid functional Becke 3-parameter exchange functional[9–11] and the Lee–Yang–Parr nonlocal correlation functional (B3LYP)[12] as implemented in the Gaussian 09, Revision D.01 software package.[13] For light atoms (H, C, N, O, and F), a polarized split-valence triple-ζ basis set that includes p functions on hydrogen atoms and d functions on other atoms (*i.e.* the 6-311G(d,p) or 6-311G** basis set) was used. A Wood-Boring[14] quasi-relativistic effective core potential (*i.e* MWB46) was used for Sb. All calculations were performed with a polarizable continuum (PCM) solvation model in toluene using a polarizable conductor calculation model (CPCM).[15,16] All geometries were confirmed as local minima structures by calculating the Hessian matrix and ensuring that no imaginary eigenvalues were present. Excited state calculations were preformed using time-dependent DFT (TD-DFT)[17–21] with the same functionals, basis sets, and solvation details as the ground state, but with the inclusion of diffuse functions on all light atoms (*i.e.* the 6-311++G(d,p) or 6-311++G** basis set). Excited state energies were computed for the 15 lowest singlet and triplet excited states. All optimized geometries and molecular orbitals were rendered in the program Avogadro.[22] Simulated UV–vis spectra were generated in the program Gauss View 5 by broadening transition lines with Gaussian functions with a half width of 0.06 eV.

X-ray Crystallographic Details

Diffraction quality crystals were obtained from a toluene solution of the compound at –30 °C in a nitrogen atmosphere glovebox, affording crystals of **2** as red plates. X-ray diffraction analysis was performed on a single crystal of **2** coated with Paratone-N oil and mounted on a glass fiber. The crystal was frozen at 100 K by an Oxford Cryosystems cryostream. Radiation was generated from a graphite fine focus sealed tube Mo Kα source (0.71073 Å). Data were collected at the Harvard Department of Chemistry and Chemical Biology X-ray Laboratory on a Bruker D8 diffractometer equipped with a Bruker APEX-II CCD detector. Raw data were integrated and corrected for Lorentz and polarization effects using Bruker AXS SAINT software.[23] Absorption corrections were applied using SADABS.[24] The structure was solved using intrinsic phasing using SHELXT[25,26] and refined using SHELXL[27,28] operated in the OLEX2[29] interface. No significant crystal decay was observed during data collection.

The crystal diffracted very poorly beyond 1.12 Å resolution, so a resolution of 0.83 Å could not be achieved. The data used for refinement was integrated to a resolution limit where intensity/sigma > 3 and R_{int} < 0.27. In addition, two strong residual electron density peaks (4.07 and 3.84 electrons/Å^3) were located close to one of the phenyl rings (C65–C70) of the SbO corrole dimer. These peaks are attributed to unresolved twinning that is aggravated by the strong scattering of the Sb centres. The lack of strong reflections precluded the identification and refinement of additional twin domains. The weak diffraction of the crystal and unresolved twinning led to a structure that is of inadequate quality for accurate determination of bond distances and angles. Thus, only the overall connectivity and arrangement of molecules should be interpreted from the structure.

While four toluene solvent molecules were located and modeled in the structure, a small portion of the structure contains electron density that could not be modeled. This electron density likely arises from severely disordered toluene solvent molecules. Consequently, the unassigned electron density was accounted for using SQUEEZE[30] as implemented in the PLATON interface. As a result of the low resolution and unresolved twinning, a stable refinement was only achieved by using strong atomic displacement restraints (RIGU, SIMU, and in select cases EADP) on the SbO corrole dimer. Geometric constraints (AFIX) were applied to the phenyl ring (C65–C70) close to the strong residual electron density peaks. Atomic displacement parameter restraints (RIGU and SIMU) as well as geometric constraints (AFIX) were also applied to the toluene solvent molecules in the crystal. One toluene molecule was found to be disordered over two positions. The relative occupancies of each of these positions were refined against each other (53(2):47(2)) and then fixed in the final refinement. The disordered toluene molecule required additional distance (DFIX and SADI) and geometric (FLAT) restraints. Hydrogen atoms were placed in ideal positions and refined using the riding model. The structure gives rise to A and B level alerts from

checkCIF. Responses addressing these alerts have been included in the CIF and can be read in reports generated by checkCIF.

Unit cell parameters and solution statistics for the structure are summarised in Table S1. Thermal ellipsoid plots are drawn at the 50% probability level with hydrogen atoms and solvent molecules removed for clarity.

NMR Spectral Details

All NMR spectra were recorded in $CDCl_3$ at 25 °C at 500 MHz for ^{1}H spectra, 470 MHz for ^{19}F spectra, or 100 MHz for ^{13}C spectra. The ^{1}H, ^{19}F, and ^{13}C spectra of **2** are presented on the following pages.

^{1}H NMR spectrum of **2**

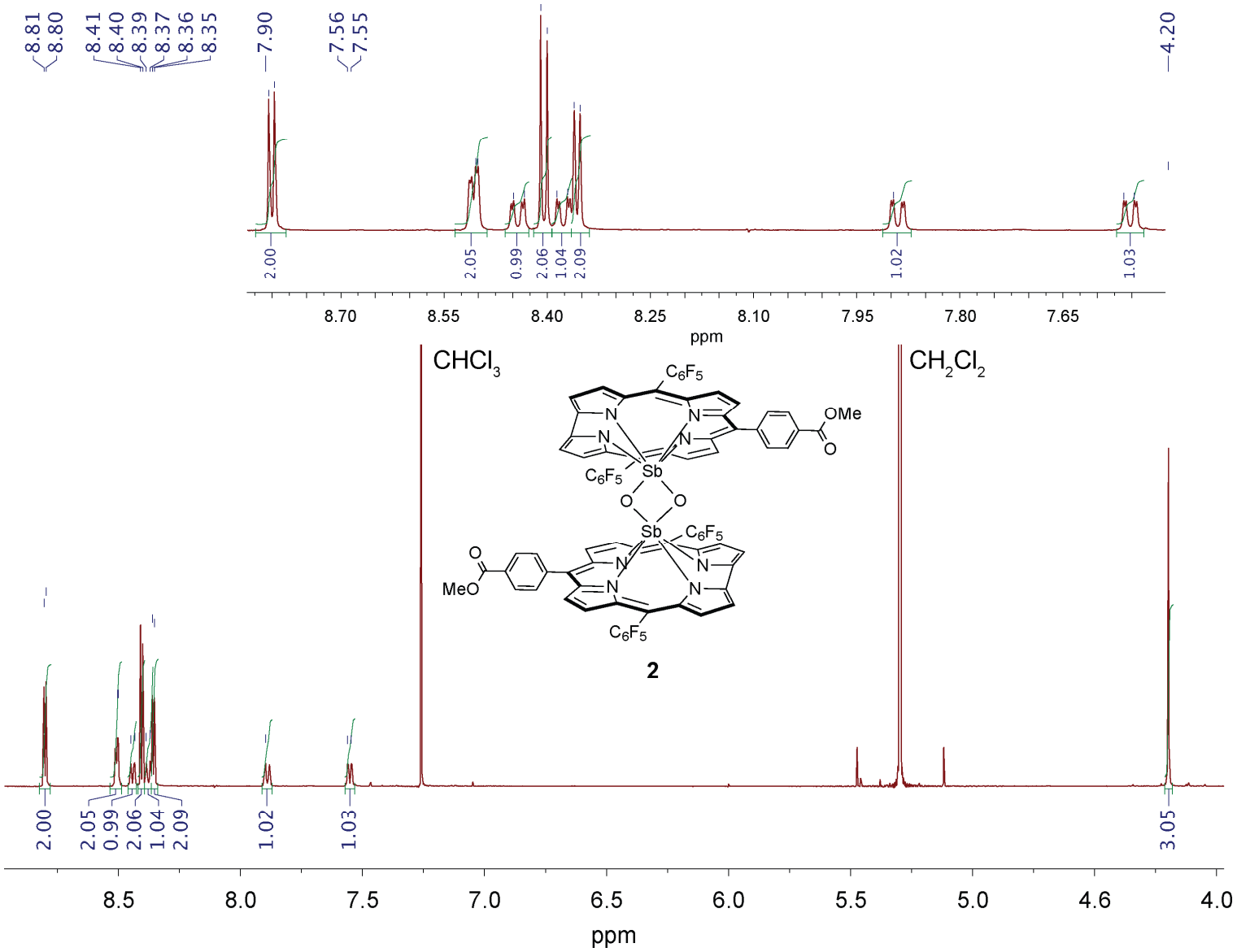

^{19}F NMR spectrum of **2**

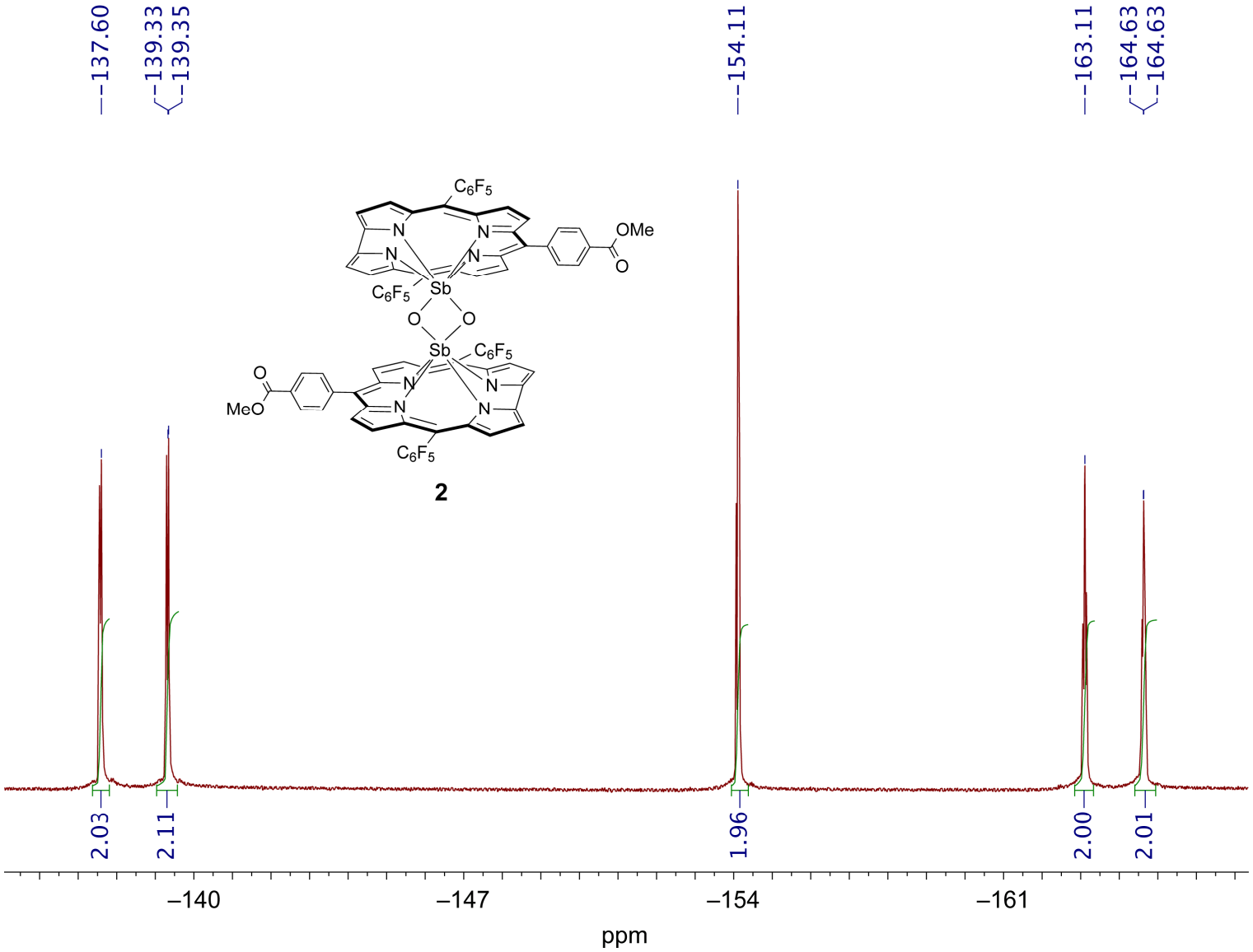

^{13}C NMR spectrum of **2**

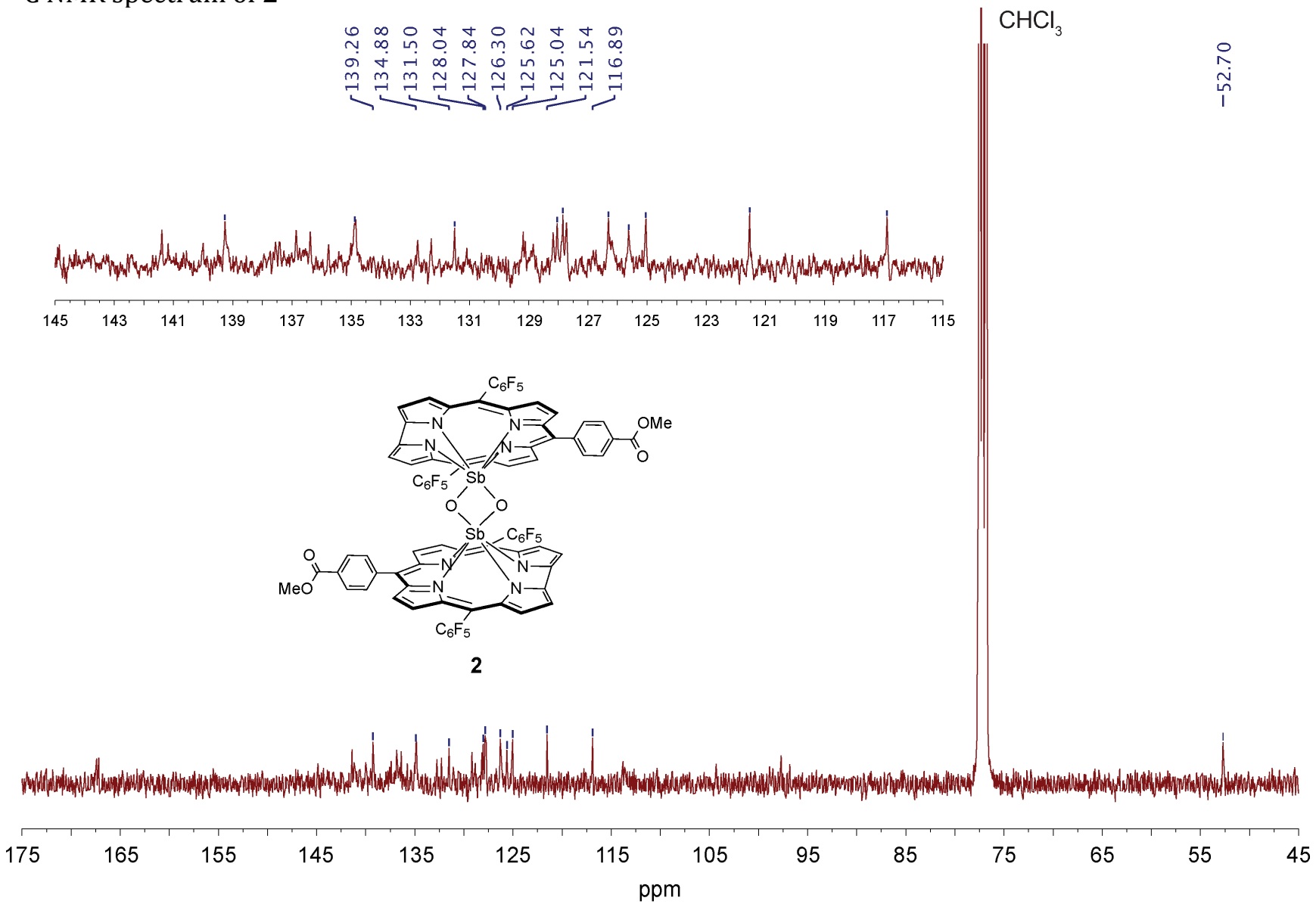

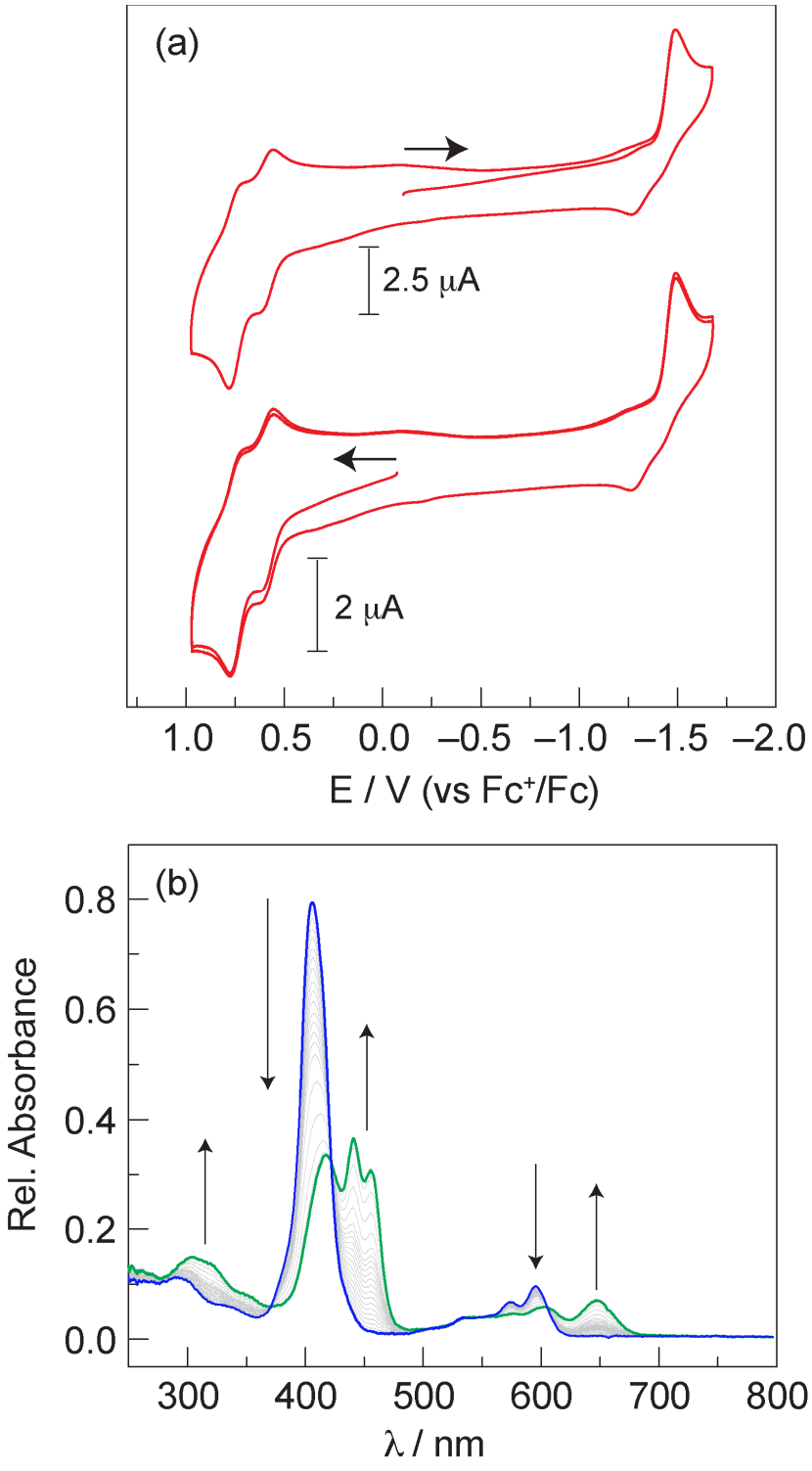

Figure S1. (a) Cyclic voltammogram of **2** in MeCN with 0.1 M [TBA][PF_6] recorded at 100 mV/s under a nitrogen atmosphere. Identical CVs are obtained when the initial scan is run in the cathodic or anodic direction. (b) Spectroelectrochemistry of **2** with bulk electrolysis conducted at –1.8 V vs. Fc^+/Fc, showing the reduction to **1**.

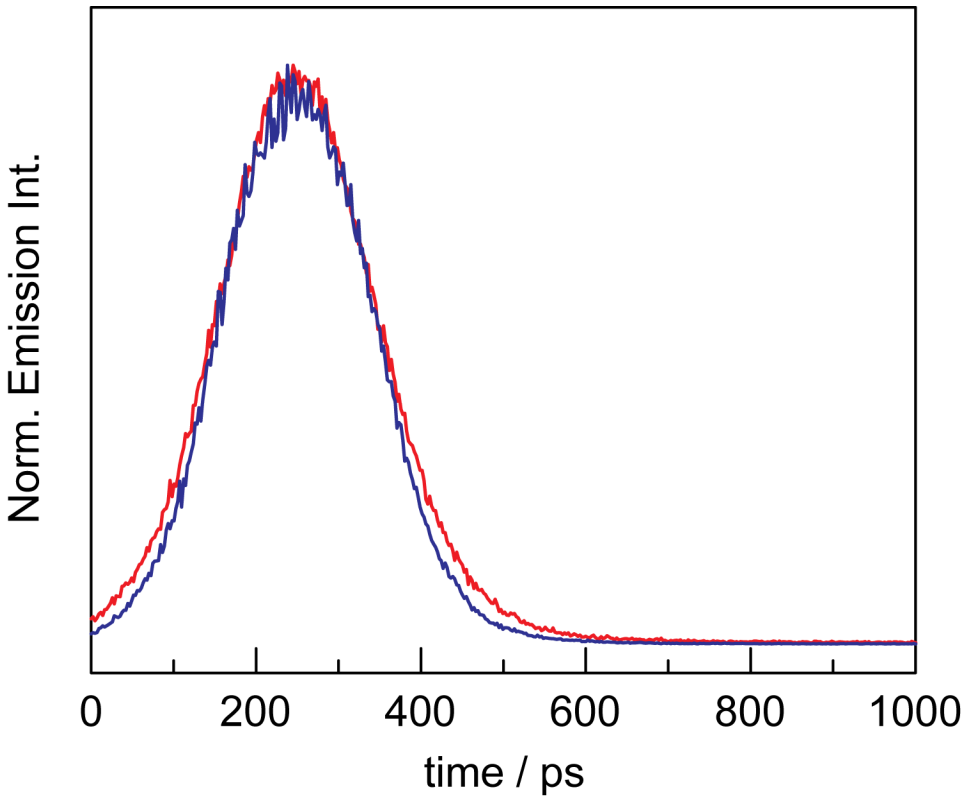

Figure S2. Fluorescence decay trace for **2** (—) in aerated toluene. Since this trace is on the order of the instrument response function (—), it is not possible to extract meaningful lifetimes from this data. As a result, the fluorescence lifetimes are estimated to be < 80 ps. This value represents the return of the signal to baseline (~400 ps), assuming that this process takes five lifetimes.

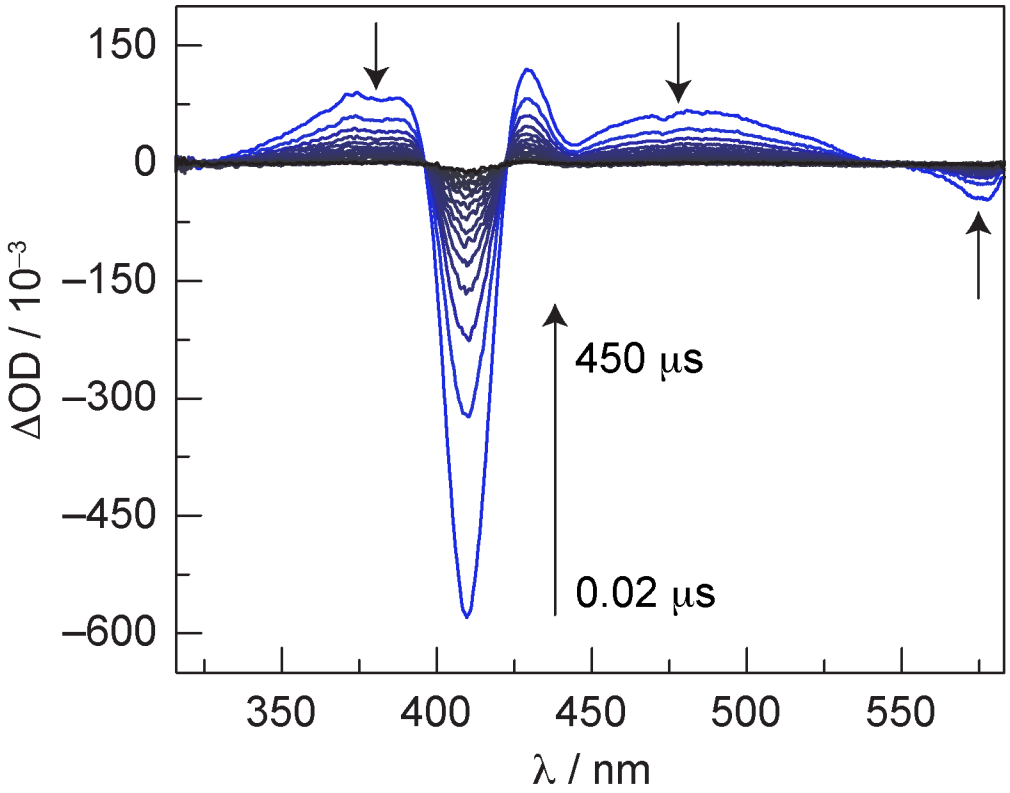

Figure S3. Nanosecond transient absorption (TA) spectra (λ_{exc} = 600 nm) of a freeze–pump–thawed toluene solution of **2**, showing the bleach of the ground state with concomitant growth of the triplet state. Temporal evolution is from 20 ns (prompt spectrum) to 450 μs in 30 μs intervals.

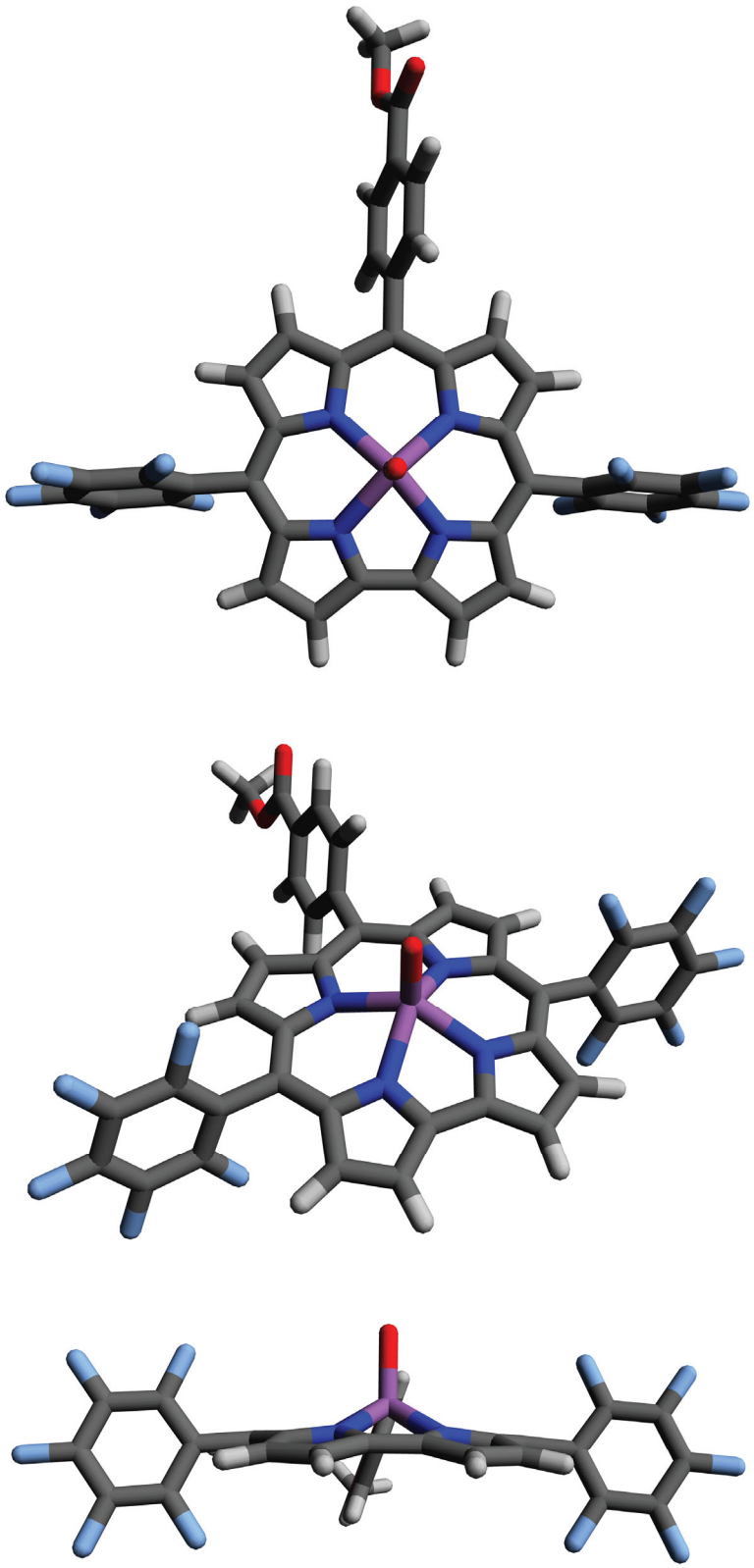

Figure S4. DFT-optimized geometry of **2** monomer using the 6-311G** basis set.

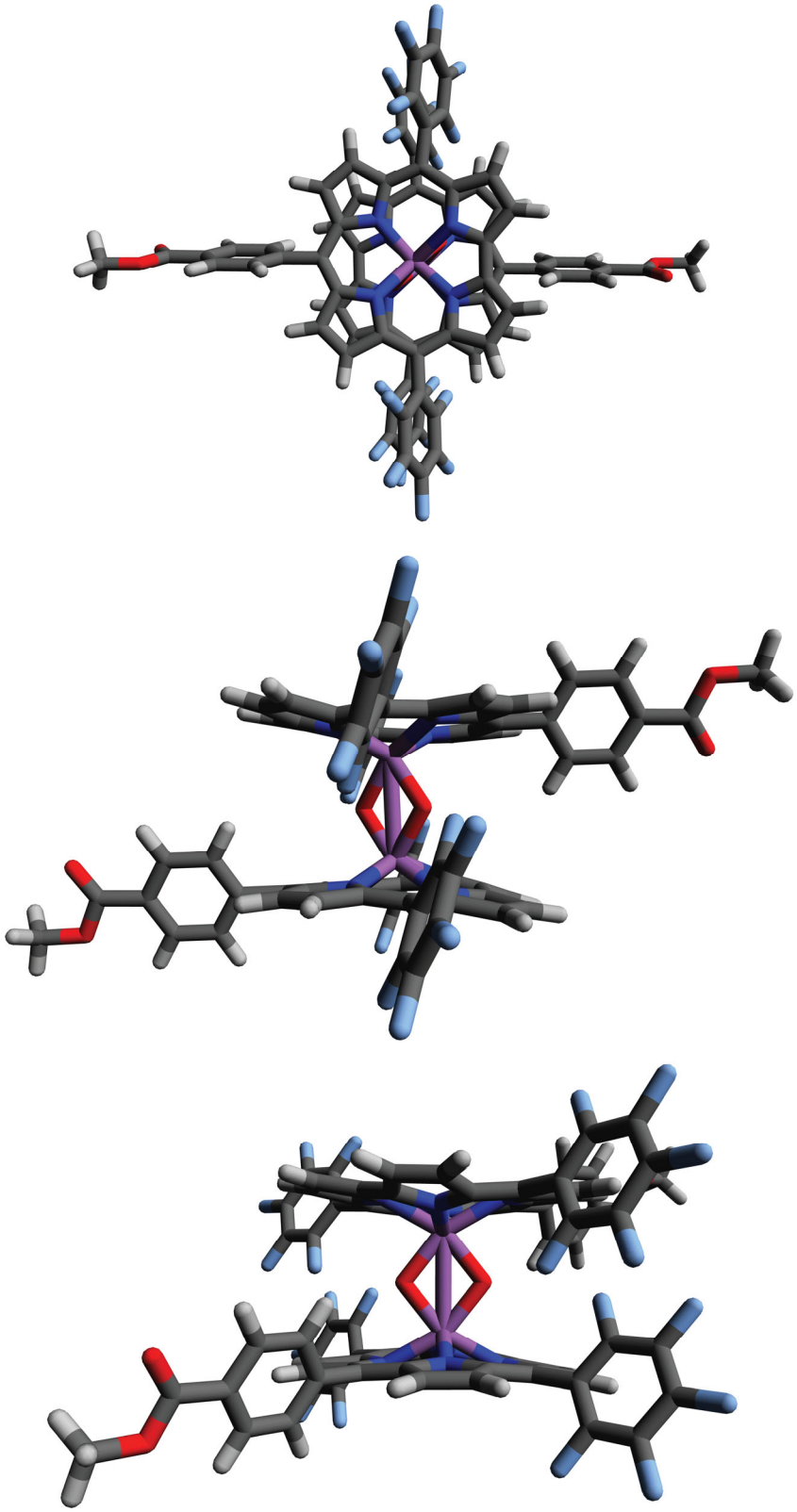

Figure S5. DFT-optimized geometry of **2** using the 6-311G** basis set.

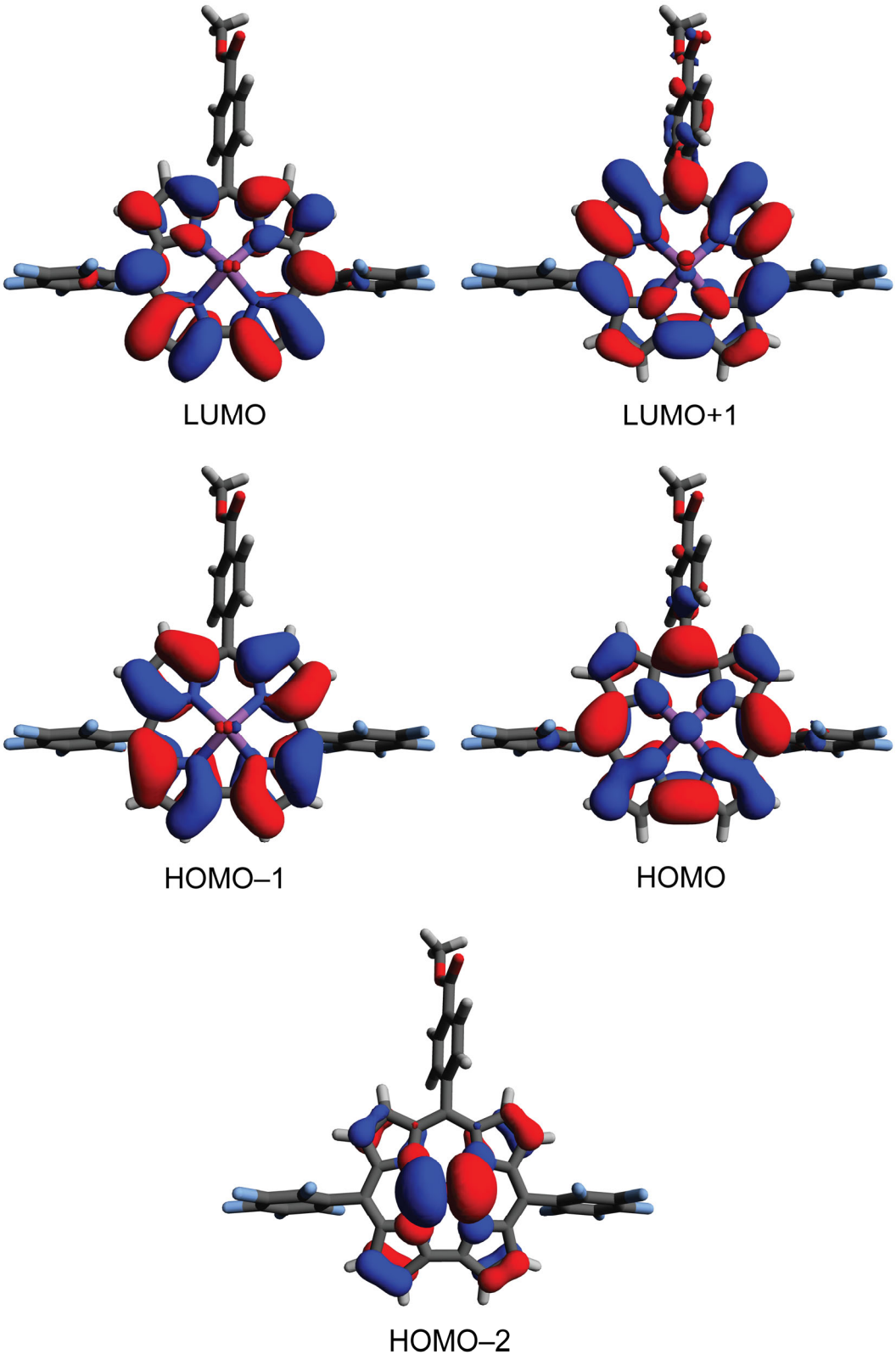

Figure S6. Frontier molecular orbitals of **2** monomer.

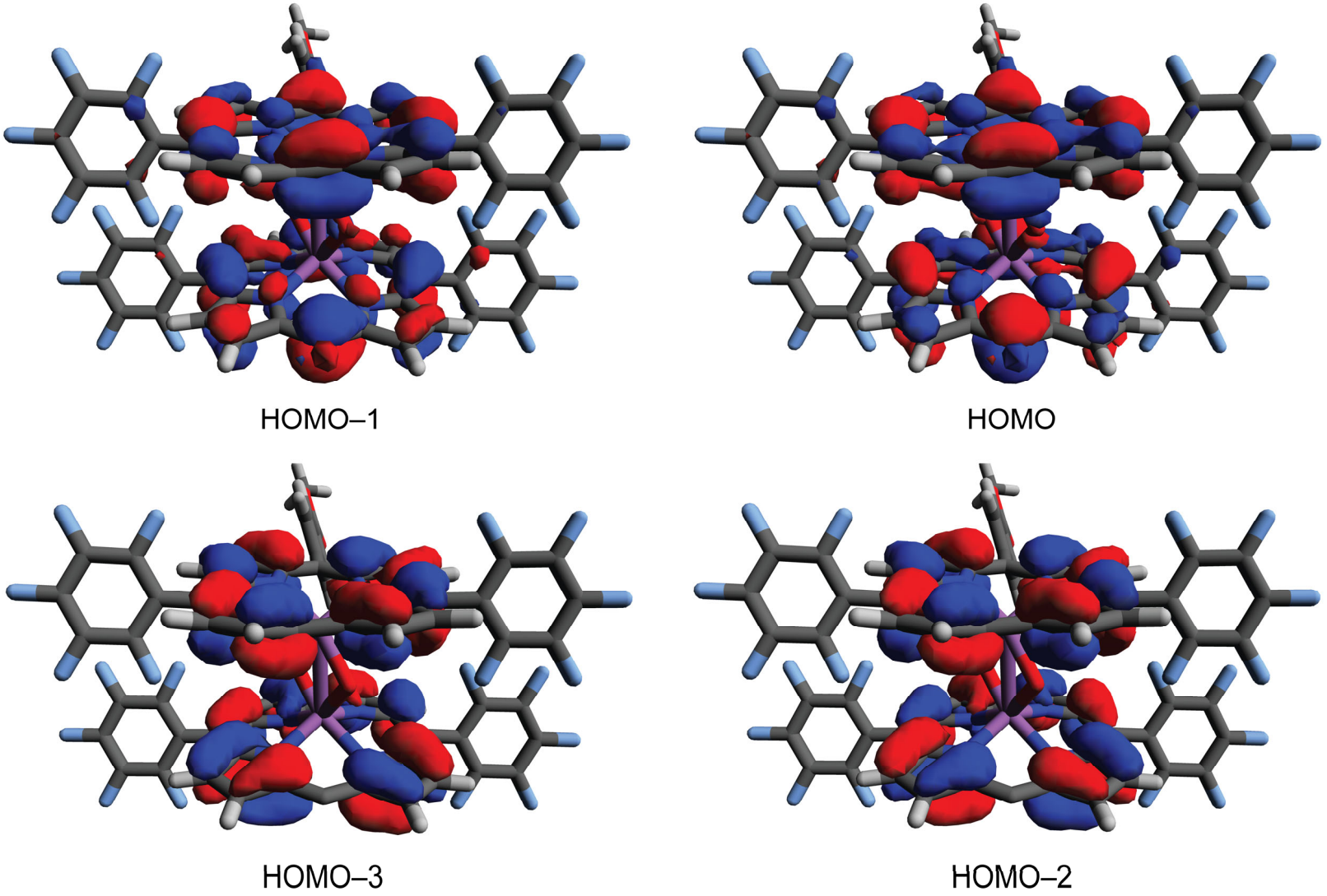

Figure S7. The four highest occupied molecular orbitals of **2**. Both HOMO–3 and HOMO–2 of the dimer are comparable to the HOMO–1 of **2** monomer, whereas HOMO–1 and HOMO are similar to the HOMO of **2** monomer. One of the 10-aryl substituents has been removed for clarity.

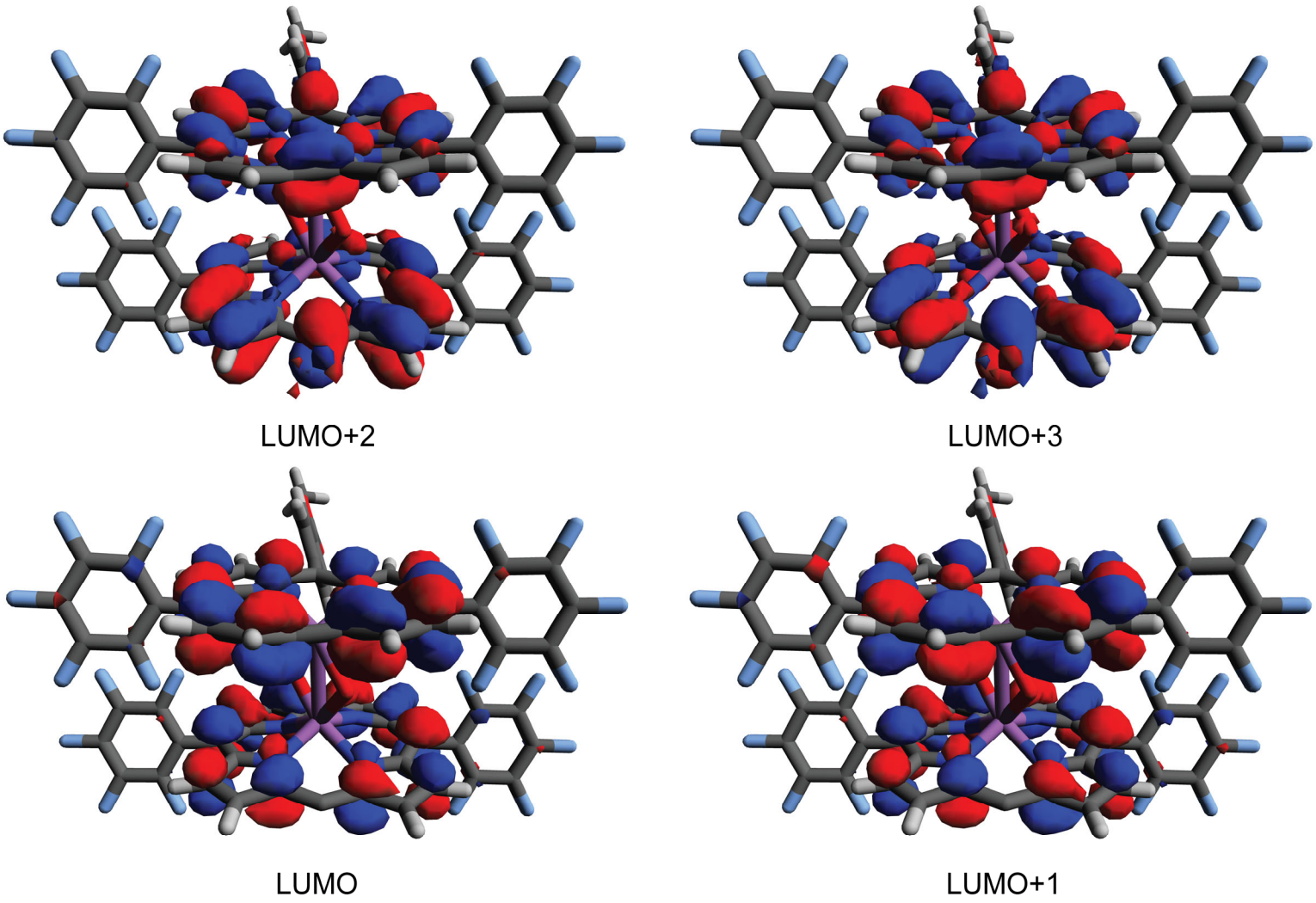

Figure S8. The four lowest unoccupied molecular orbitals of **2**. Both LUMO and LUMO+1 of the dimer are comparable to the LUMO of **2** monomer, whereas LUMO+2 and LUMO+3 are similar to the LUMO+1 of **2** monomer. One of the 10-aryl substituents has been removed for clarity.

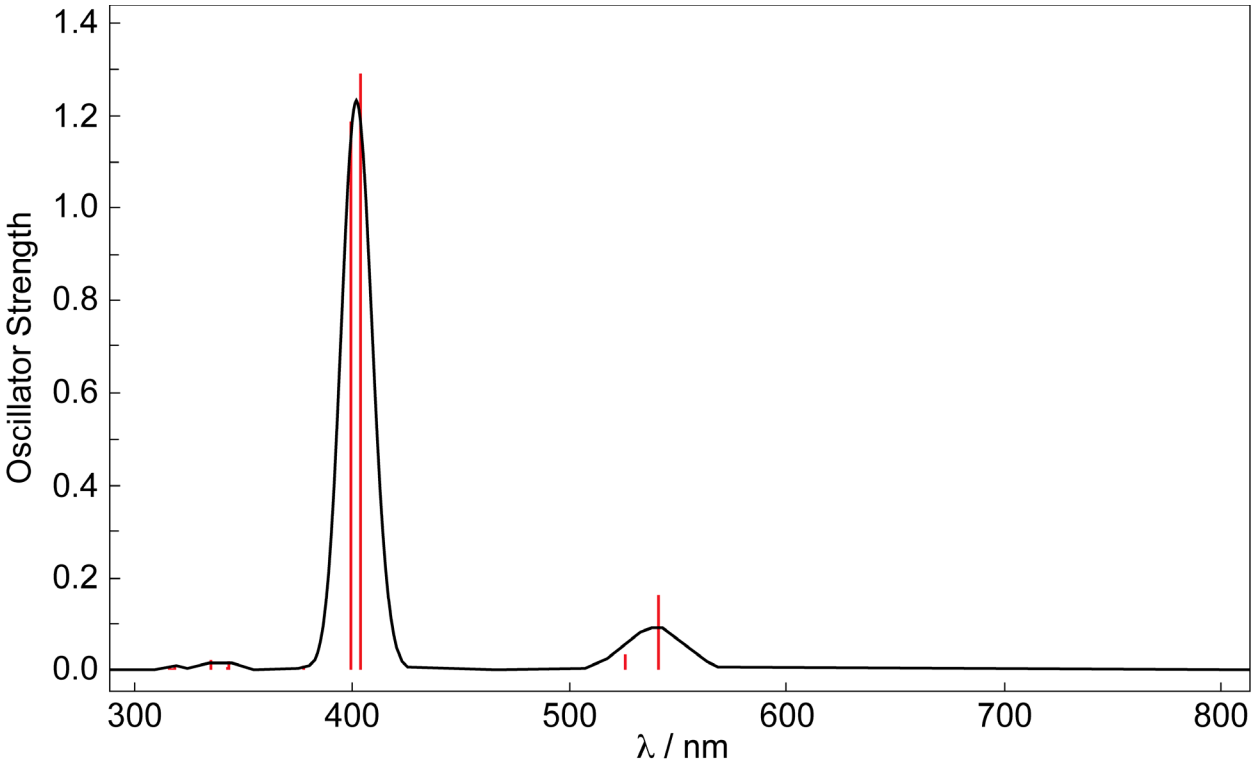

Figure S9. Simulated UV-vis spectrum of **2** monomer. The transition lines have been broadened with Gaussian functions that have a half width of 0.06 eV.

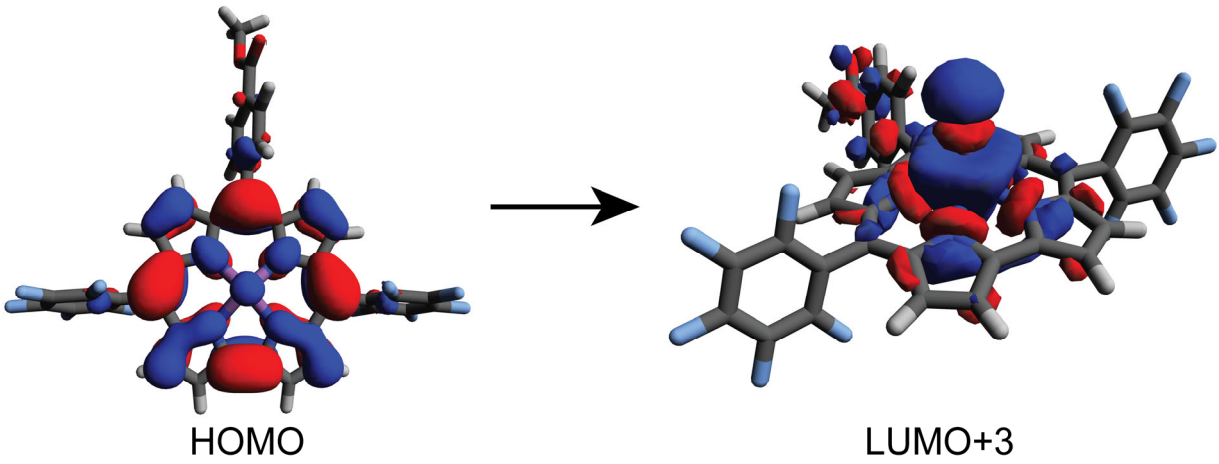

Figure S10. Illustration of the primary (87%) orbital transition associated with S_5 of compound **2** monomer that corresponds to the UV absorption bands to the blue of the Soret band.

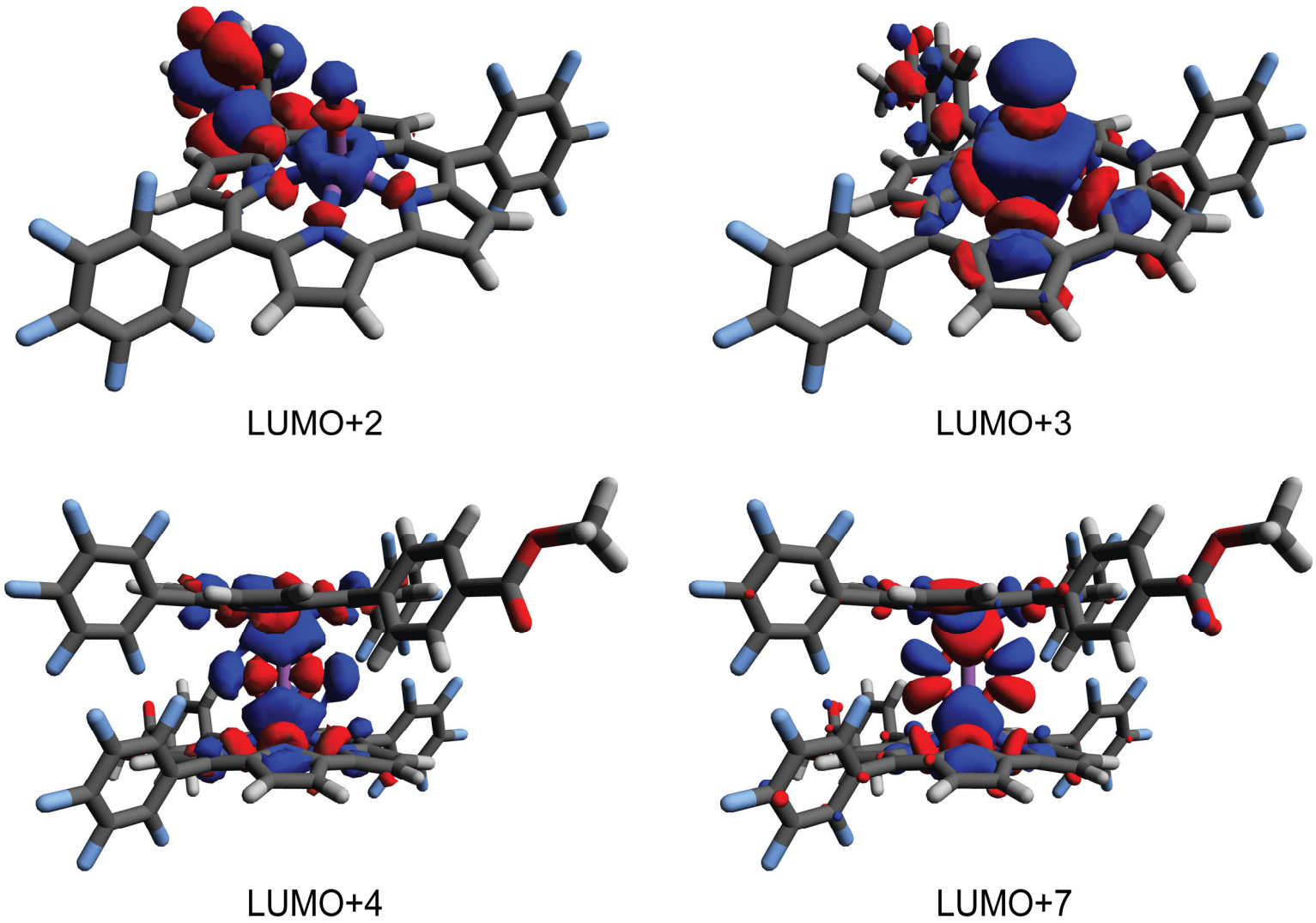

Figure S11. Unoccupied orbitals of **2** monomer (LUMO+2, LUMO+3) and **2** (LUMO+4, LUMO+7) that exhibit antibonding character with respect to the Sb–O bond. These orbitals are populated in the UV transitions to the blue of the Soret band.

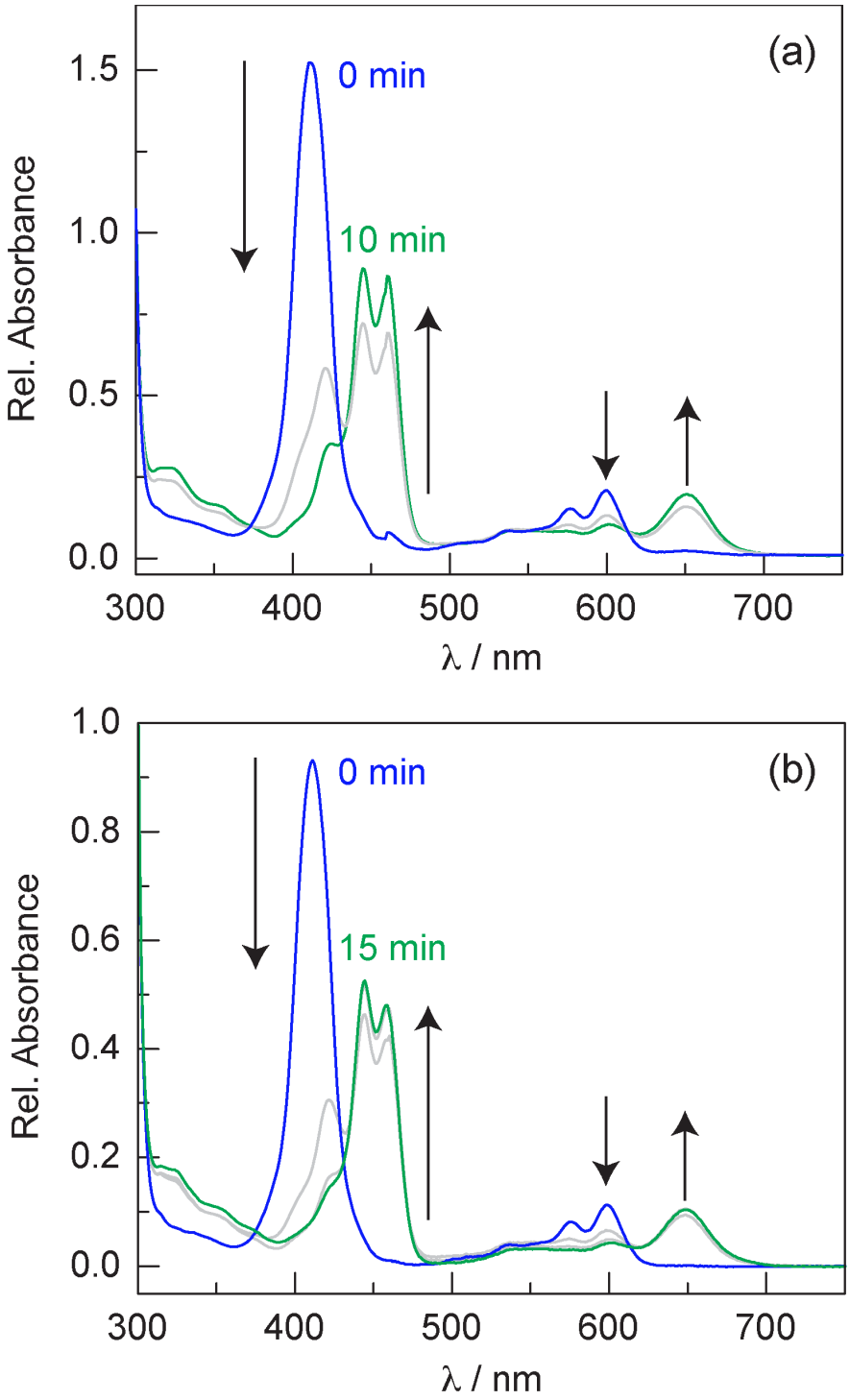

Figure S12. (a) Photolysis (λ_{exc} > 305 nm) of a sample of **2** in toluene in the presence of 1,3-cyclohexadiene. The initial spectrum of **2** (—) evolves to that of **1** (—) over the course of 10 min. Spectra were recorded every 5 min. (b) Photolysis (λ_{exc} > 305 nm) of a sample of **2** in benzene in the presence of 1,3-cyclohexadiene. The initial spectrum of **2** (—) evolves to that of **1** (—) over the course of 15 min. Spectra were recorded every 5 min.

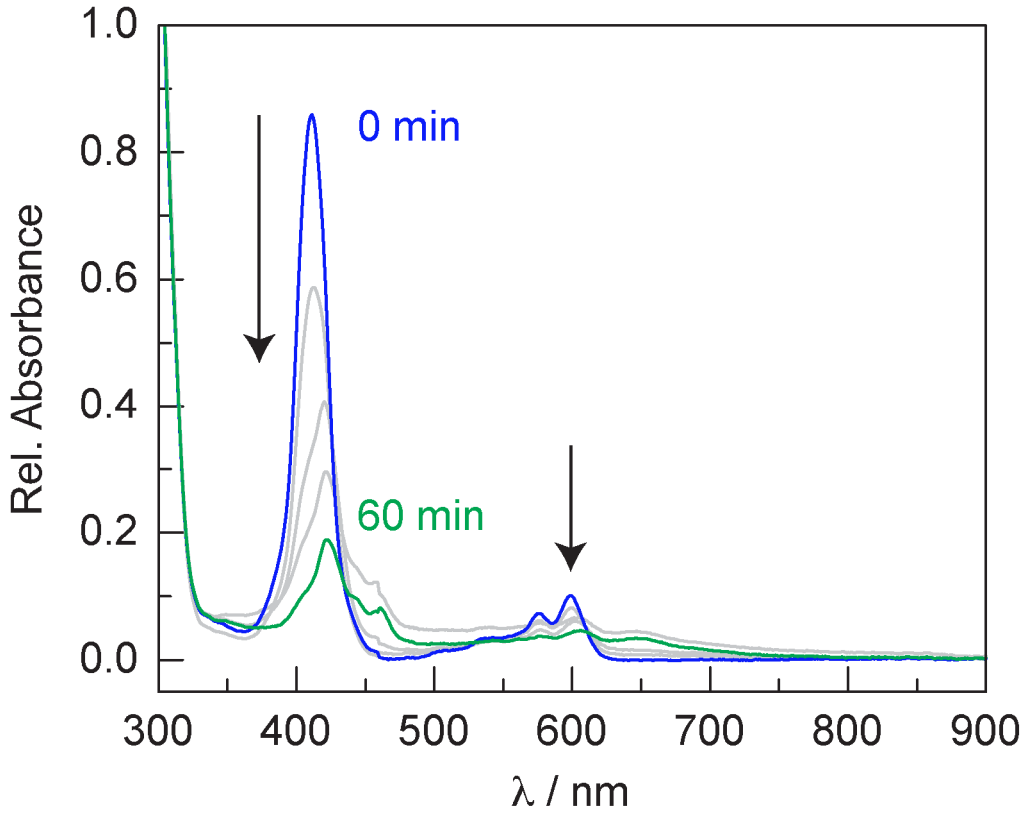

Figure S13. Photolysis (λ_{exc} > 305 nm) of a sample of **2** in benzene. The initial spectrum of **2** (—) evolves over the course of 1 h (—). Spectra were recorded every 15 min. Given the high BDE of benzene (112.9 kcal/mol), photogenerated radicals react with the weaker C–H bonds of the corrole, resulting in decomposition of **2**. This result indicates that benzene is an unreactive substrate.

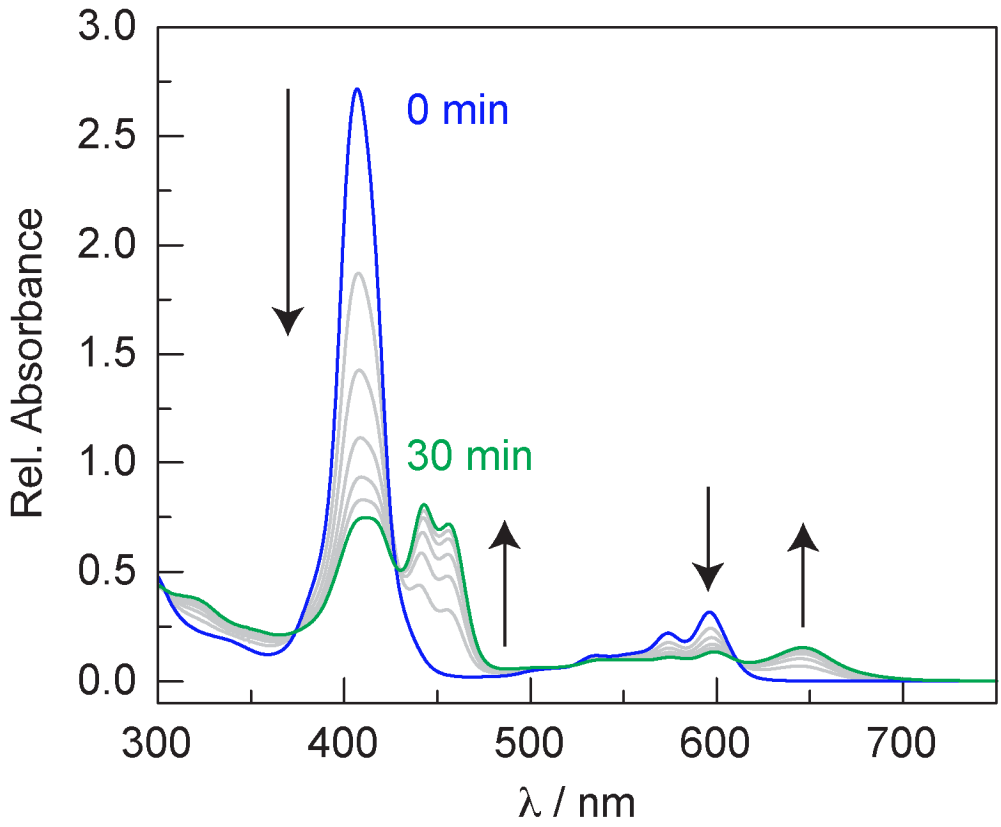

Figure S14. Photolysis (λ_{exc} > 305 nm) of a sample of **2** in THF. The initial spectrum of **2** (—) evolves to that of **1** (—) over the course of 30 min. Spectra were recorded every 5 min.

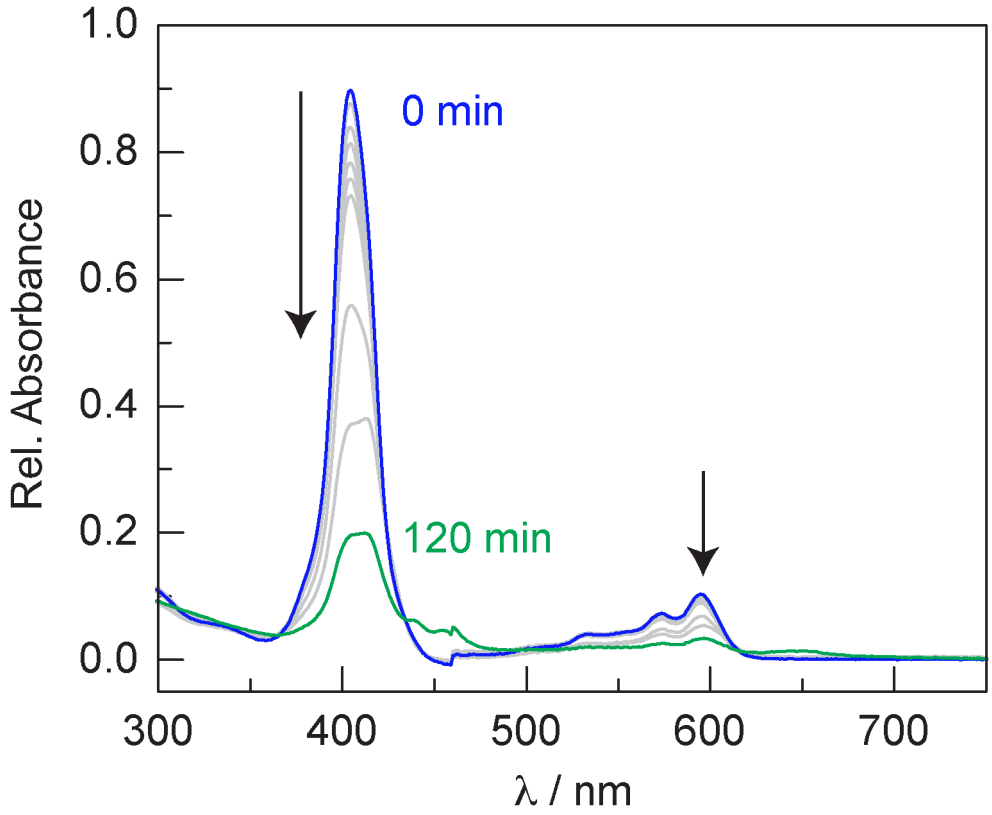

Figure S15. Photolysis (λ_{exc} > 305 nm) of a sample of **2** in MeCN. The initial spectrum of **2** (—) evolves over the course of 2 h (—). Spectra were recorded every 5 min for the first 30 min, then every 30 min for the next 1.5 h.

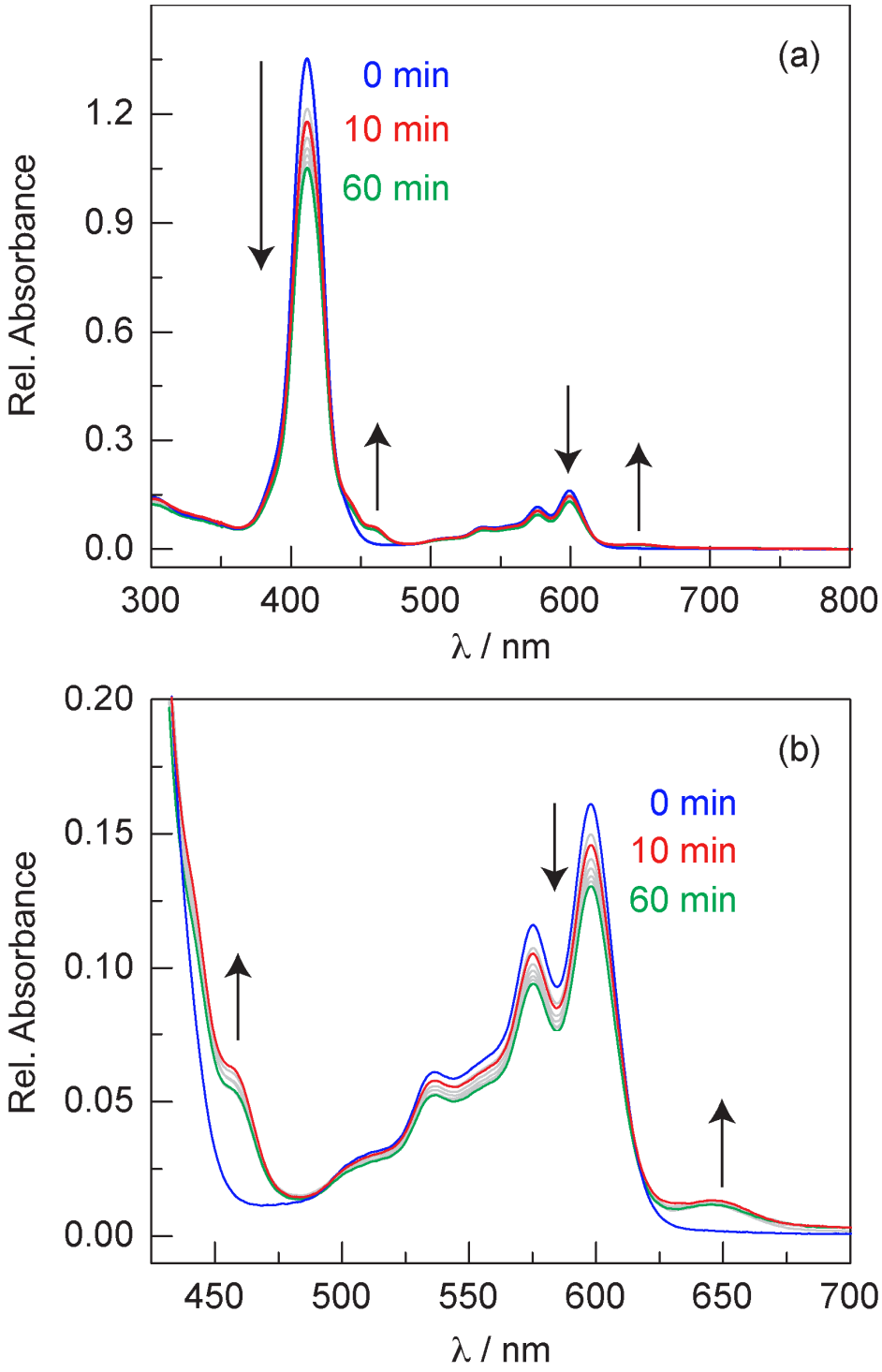

Figure S16. (a) Photolysis (λ_{exc} > 305 nm) of a sample of **2** in a 1:1 mixture of benzene and 2-propanol. The initial spectrum of **2** (—) evolves over the course of 1 h (—). Spectra were recorded after 5, 10, 20, 30, 40, 50, and 60 min of photolysis. After 10 min (—), the photochemical generation of **1** ceases and the total signal of the sample decreases with subsequent photolysis. (b) Expansion of the Q band region to more clearly illustrate the spectral changes in (a).

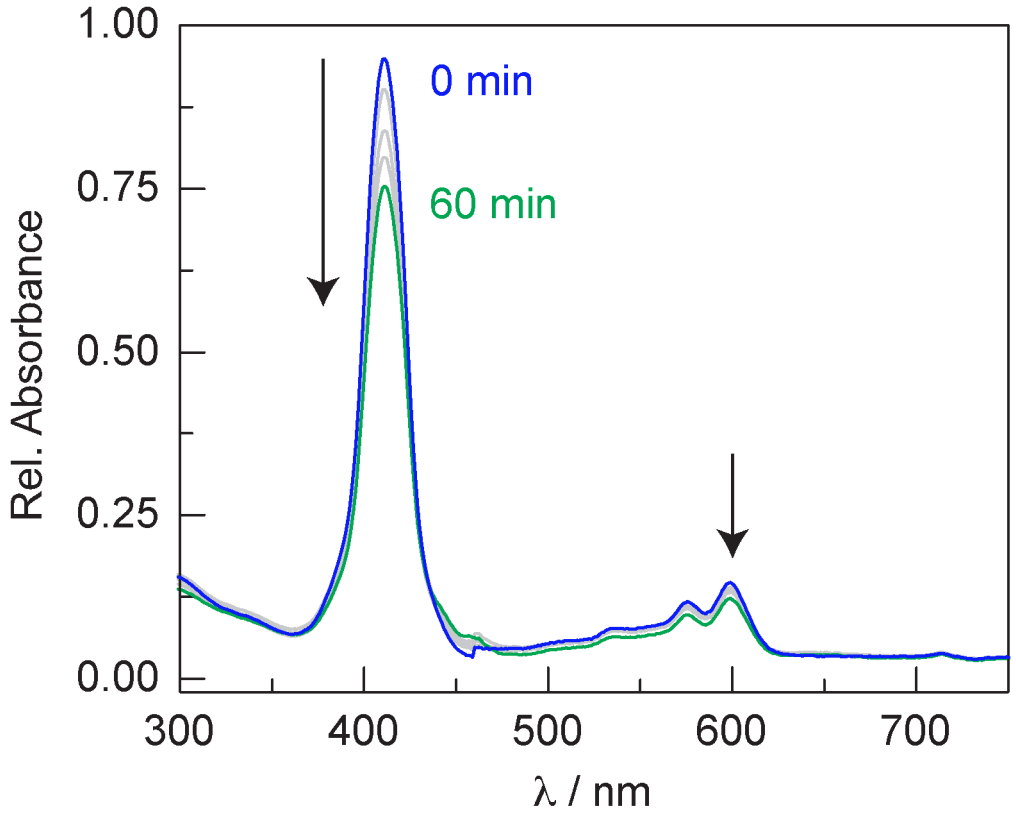

Figure S17. Photolysis (λ_{exc} > 305 nm) of a sample of **2** in a 1:1 mixture of benzene and cycloheptane. The initial spectrum of **2** (—) evolves over the course of 1 h (—). Spectra were recorded every 15 min.

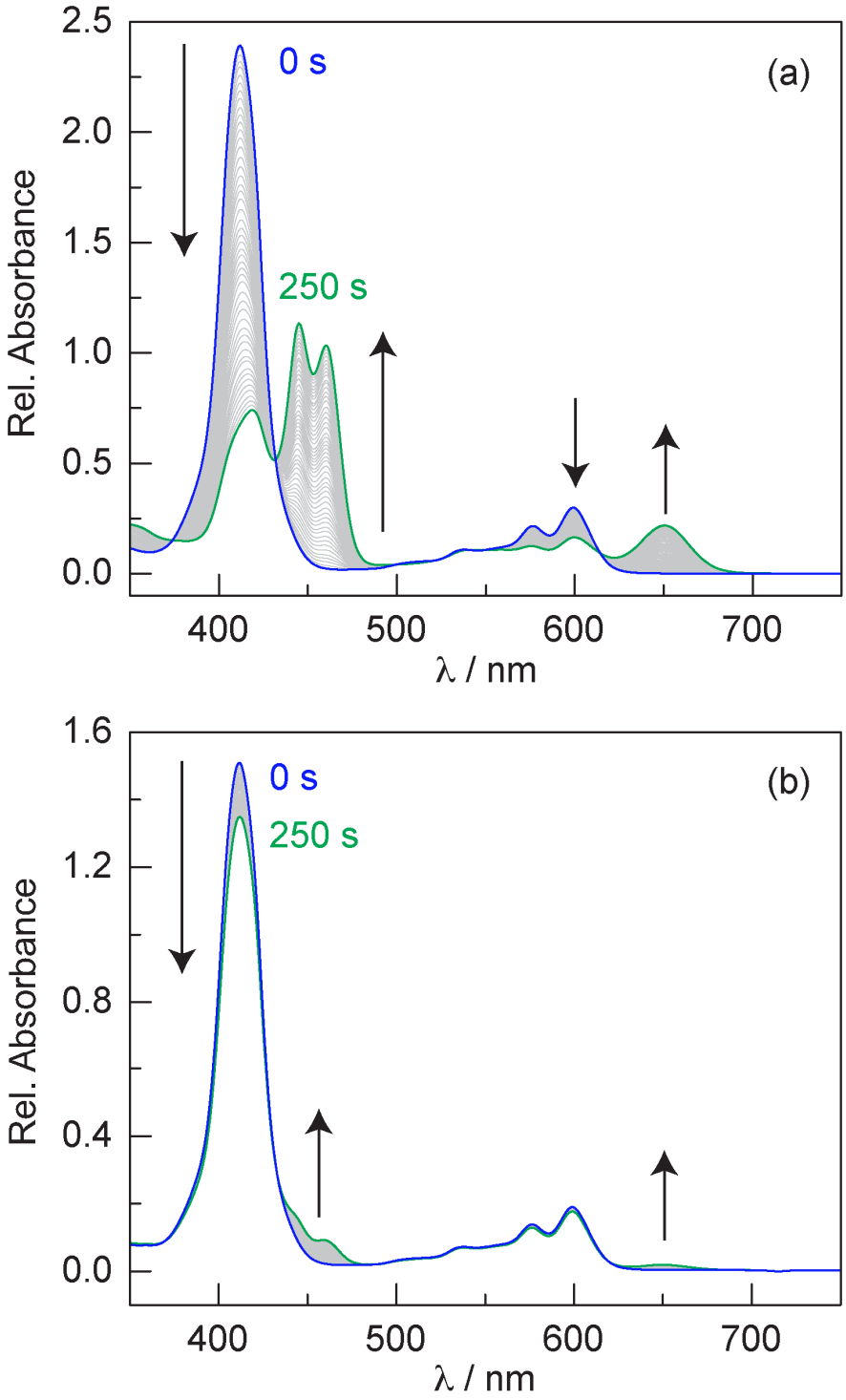

Figure S18. Photolysis (λ_{exc} > 305 nm) of a sample of **2** in (a) protic toluene and (b) toluene-d_8. In both cases, the initial spectrum of **2** (—) evolves over the course of 250 s (—) and spectra were recorded every 5 s. After 250 s, the conversion to **1** is 50% complete in protic toluene, but only 7% complete in toluene-d_8.

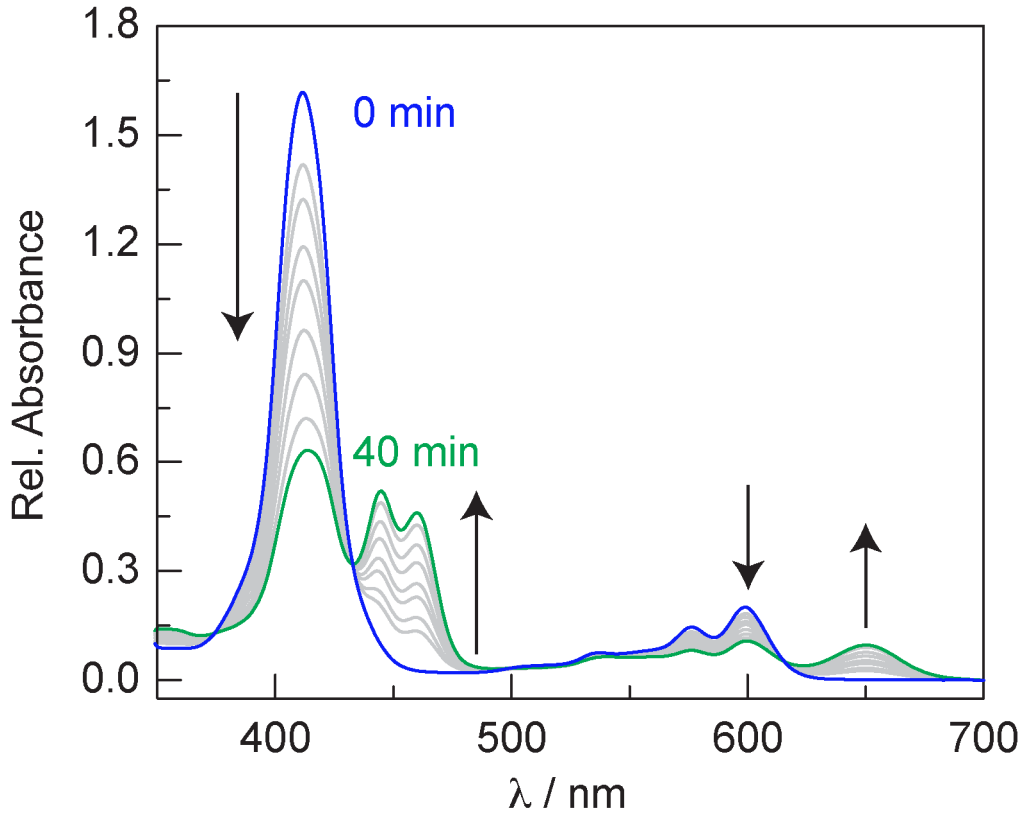

Figure S19. Photolysis (λ_{exc} > 305 nm) of a sample of **2** in toluene-d_8. The initial spectrum of **2** (—) evolves over the course of 40 min (—). Spectra were recorded every 5 min. After 40 min, the conversion to **1** is 32% complete.

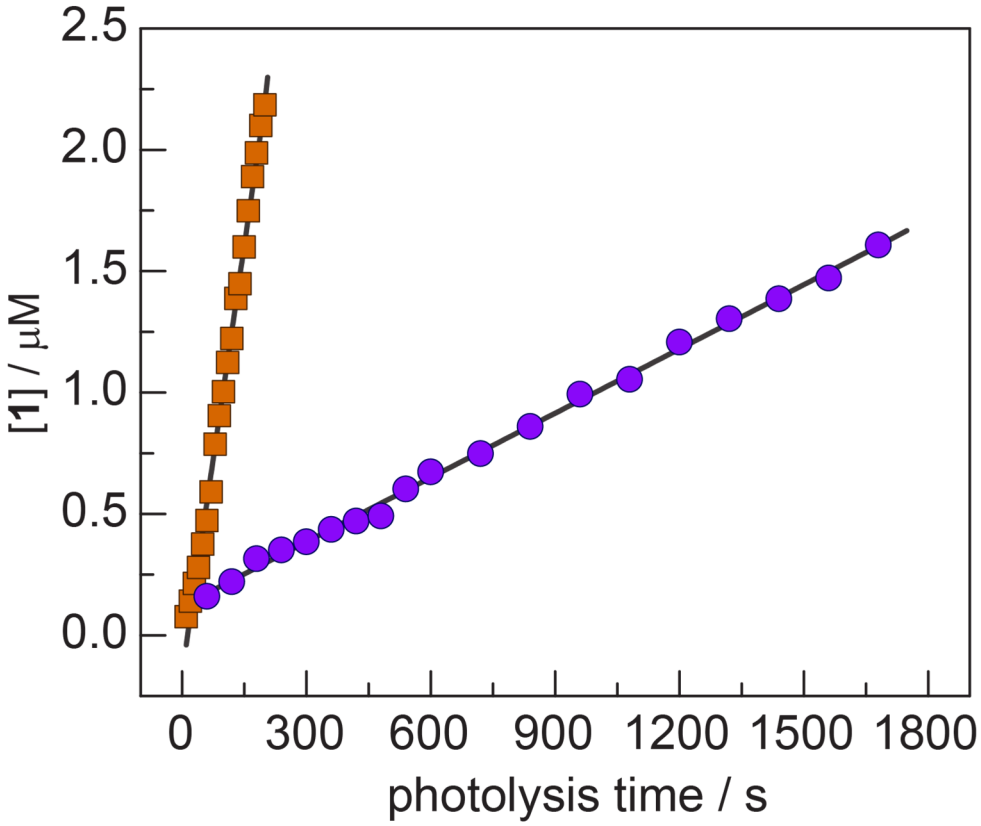

Figure S20. Conversion of **2** to **1** in protic (■) and deuterated (●) toluene as a function of photolysis time, monitoring the growth of the absorption at 650 nm. This data yields rate constants of k_{obs} = 1.17 × 10^{-8} M s^{-1} for protic toluene and k_{obs} = 8.83 × 10^{-10} M s^{-1} for deuterated toluene.

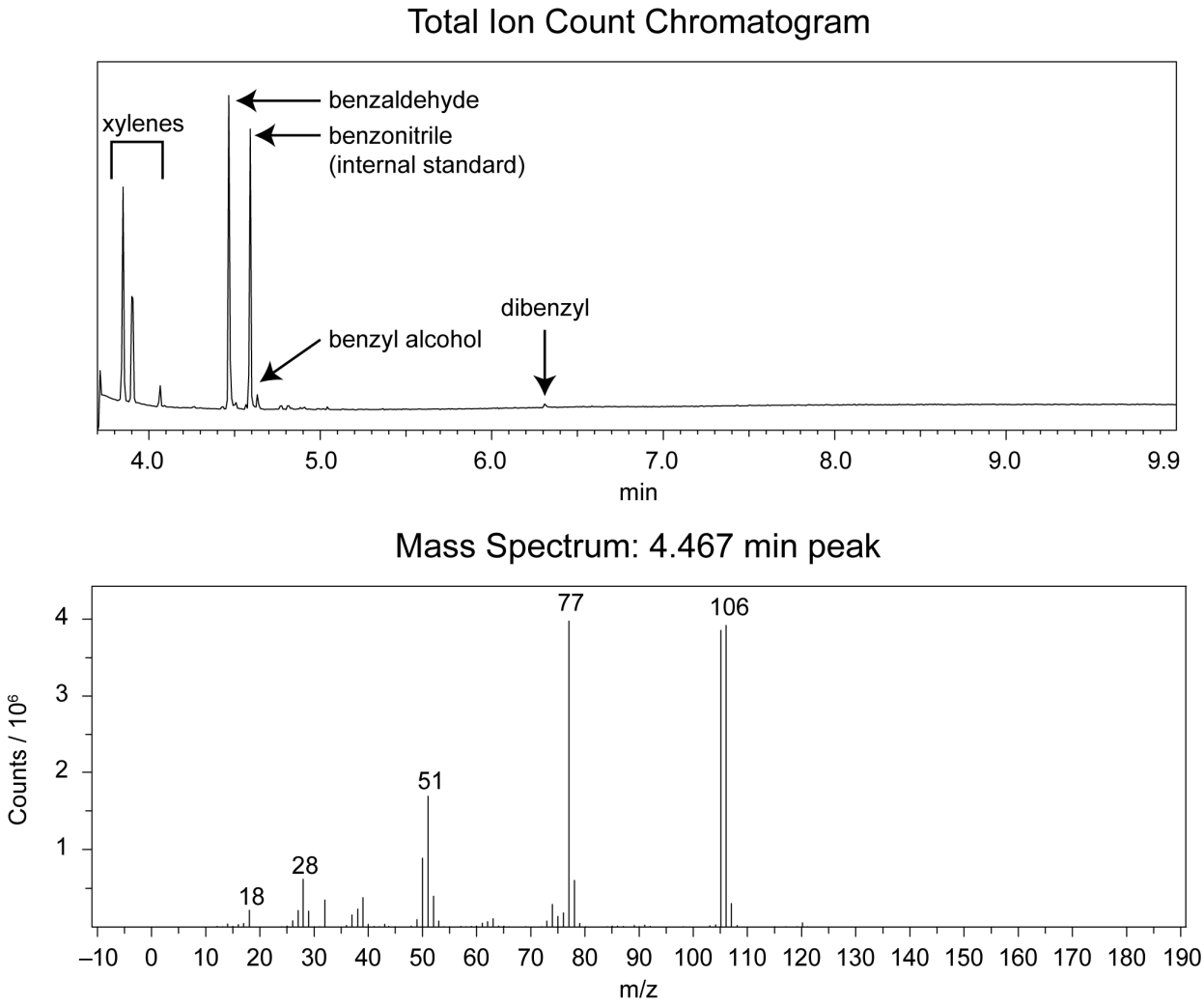

Figure S21. GC-MS analysis from a sample of **2** that was photolyzed (λ_{exc} > 305 nm) in toluene. The top trace shows the total ion count chromatogram. The observation of xylenes in the sample is due to the presence of these species in the toluene solvent. Benzaldehyde (peak at 4.47 min) was identified on the basis of the mass spectrum (lower trace) and confirmed by running a standard of the compound.

Table S1. Summary of Crystallographic Data for Compound **2**

	2
Formula	$C_{106}H_{62}F_{20}N_8O_6Sb_2$
Weight (g/mol)	2167.13
Temperature (K)	100(2)
Crystal System	Monoclinic
Space Group	$P2_1/c$
Color	Red
a (Å)	14.7806(17)
b (Å)	19.611(2)
c (Å)	32.180(4)
α (°)	90
β (°)	100.277(2)
γ (°)	90
V (Å^3)	9177.8(19)
Z	4
No. Reflections	38130
No. Unique Refl.	6846
R_{int}	0.1222
$R1^a$ (all data)	0.1223
$wR2^b$ (all data)	0.2333
$R1$ [(I > 2σ)]	0.0818
$wR2$ [(I > 2σ)]	0.2031
GOF^c	1.023

^{a} $R1 = (\Sigma||F_o| - |F_c||)/\Sigma|F_o|$. ^{b} $wR2 = [\Sigma w(F_o^2 - F_c^2)^2/\Sigma wF_o^2]^{1/2}$. ^{c} GOF = $[\Sigma w(F_o^2 - F_c^2)^2/(n - p)]^{1/2}$ where n is the number of independent reflections and p is the number of refined parameters.

Table S2. Cartesian coordinates for the DFT optimized geometry for **2** monomer (E = –2944.33442498 hartrees)

	x	*y*	*z*
C	0.69485168	–3.75067150	0.12409106
C	1.76213544	–4.63395433	0.42261419
C	2.93730843	–3.90054377	0.35871542
C	2.60267666	–2.54940295	0.03404635
N	1.24289056	–2.51600373	–0.12942884
H	1.66519132	–5.67695034	0.68123465
H	3.93154546	–4.26632211	0.56342193
C	3.35996105	–1.36312608	0.00430379
C	2.78833034	–0.08083765	–0.06333189
C	1.24870269	1.59515995	–0.09054017
C	2.54824588	2.17905189	0.02149592
H	4.54026962	1.27590169	0.15327331
H	2.74346928	3.23563747	0.10518703
C	3.47271004	1.16896099	0.04248737
N	1.42127255	0.21553007	–0.15249809
C	0.00432640	2.25119400	–0.08904700
C	–1.24396312	1.60191779	–0.08850930
C	–2.79478704	–0.06220005	–0.04981864
C	–3.46631711	1.19024748	0.10135897
H	–2.71437827	3.24769583	0.21206038
H	–4.52878268	1.30174767	0.25009756
C	–0.72305379	–3.74603221	0.12331649
C	–2.62347689	–2.53245405	0.03633804
C	–2.96584421	–3.88155959	0.36156706
H	–1.70452591	–5.66566765	0.68312973
H	–3.96187977	–4.24101169	0.56859032
N	–1.26362586	–2.50800182	–0.13176082
N	–1.42953778	0.22636611	–0.17043161
C	–2.53379110	2.19297267	0.08208632
C	–1.79538436	–4.62234773	0.42362418
C	–3.37357443	–1.34158708	0.01694802
C	–4.85514864	–1.43648197	0.15726926
C	–5.69907577	–1.24959744	–0.93792029
C	–5.45676255	–1.72519167	1.38205347
C	–7.08012933	–1.34448150	–0.82548289
C	–6.83495548	–1.82931412	1.51741164
C	–7.64822598	–1.63682811	0.40795989
C	0.00037535	3.74692234	–0.03743145
C	–0.40537785	4.49188407	–1.15268606
C	0.39158240	4.42622664	1.12357230
C	–0.41541246	5.88020087	–1.10856033

H	–0.70443136	3.97749994	–2.05835539
C	0.38178089	5.81581630	1.17085004
H	0.69457020	3.86067992	1.99701949
C	–0.02181540	6.55253078	0.05245366
H	–0.72294554	6.45956725	–1.96998189
H	0.68112920	6.33177586	2.07325832
C	4.84242630	–1.46812791	0.12875207
C	5.45443644	–1.74251448	1.35158766
C	5.67583748	–1.30819934	–0.97853967
C	6.83294921	–1.85770230	1.47393400
C	7.05714198	–1.41437217	–0.87929169
C	7.63584784	–1.69154247	0.35272629
F	–7.86394016	–1.16086499	–1.89289672
F	–8.97362205	–1.73293674	0.52728016
F	–7.38315649	–2.10803119	2.70505390
F	–4.70018302	–1.90998459	2.47326412
F	–5.18171664	–0.96718561	–2.13984998
F	5.14797648	–1.04069904	–2.17926100
F	7.83104709	–1.25558713	–1.95786850
F	8.96155273	–1.79812710	0.45953303
F	7.39134101	–2.12250417	2.66004308
F	4.70758708	–1.90355271	2.45323952
C	–0.05164702	8.04361473	0.04464430
O	–0.40014220	8.71414290	–0.90140430
O	0.35536182	8.57175649	1.21400218
C	0.35788086	10.01099155	1.28906089
H	–0.64807445	10.40164284	1.13154312
H	1.02899900	10.42920583	0.53799096
H	0.70844584	10.24824801	2.29041919
O	0.00143387	–1.06039018	–2.80594731
Sb	–0.00500761	–1.06912605	–0.96048533

Table S3. Cartesian coordinates for the DFT optimized geometry for **2**

(E = –5888.72409771 hartrees)

	x	*y*	*z*
C	–3.78762916	–2.83963170	–1.42165508
C	–2.92918069	–3.81677673	–1.00590287
C	–1.59182080	–3.35301305	–1.21672052
C	–0.40764403	–4.02344145	–0.85717846
C	0.88783034	–3.51751554	–1.06010204
C	2.13603043	–4.19355411	–0.90318883
C	3.13072880	–3.36889644	–1.36147140
C	2.53836716	–2.15902193	–1.83588926
C	3.16303940	–1.12167755	–2.54794906
C	2.45702195	–0.06479851	–3.14970847
C	2.88408252	1.00883264	–3.99444846
C	1.76921073	1.75718362	–4.33051351
C	0.65506464	1.15431380	–3.68954353
C	–0.73900991	1.37191518	–3.55637509
C	–1.75730838	2.09693757	–4.22030563
C	–2.97490787	1.57588505	–3.80541400
C	–2.71288605	0.51328012	–2.89024196
C	–3.52938212	–0.53195958	–2.41865972
C	–3.01677876	–1.73718686	–1.90768970
C	–5.00355138	–0.37105215	–2.54103203
C	–5.69022290	0.57776119	–1.78155772
C	–5.46644295	0.29655332	1.98069935
C	–7.06720375	0.73084336	–1.85824929
C	–7.79783889	–0.06130428	–2.73380528
C	–7.14448332	–1.00165884	–3.51993624
C	–5.76671500	–1.14394592	–3.41902547
C	–0.52473048	–5.37362362	–0.22680735
C	–0.13948298	–5.56678321	1.10725990
C	–0.24315516	–6.81872048	1.69926105
C	–0.73335179	–7.90662810	0.97008512
C	–1.11688703	–7.72350457	–0.36271052
C	–1.01211068	–6.46889161	–0.95249825
C	4.64513363	–1.16104459	–2.70326267
C	5.46589477	–0.29575296	–1.97986914
C	6.84948949	–0.33680016	–2.07962054
C	7.44847284	–1.24669394	–2.94040811
C	6.65939071	–2.11023650	–3.68928978
C	5.27690584	–2.05776432	–3.56523621
C	–1.76997370	–1.75654400	4.33080269
C	–2.88468899	–1.00803536	3.99459762
C	–2.45742706	0.06534084	3.14962942

C	–3.16323505	1.12230843	2.54777172
C	–2.53835237	2.15941819	1.83553199
C	–3.13045441	3.36931685	1.36086367
C	–2.13558823	4.19367944	0.90241680
C	–0.88752720	3.51743774	1.05949997
C	0.40805378	4.02310954	0.85659227
C	1.59208781	3.35257999	1.21639840
C	2.92954295	3.81613278	1.00569187
C	3.78780473	2.83894625	1.42173430
C	3.01672314	1.73669047	1.90784370
C	3.52908819	0.53147329	2.41905916
C	2.71239034	–0.51358978	2.89067702
C	2.97416433	–1.57606042	3.80608431
C	1.75644471	–2.09687532	4.22091091
C	0.73832744	–1.37187768	3.55666936
C	–0.65571612	–1.15404478	3.68968374
C	–4.64528371	1.16210594	2.70333556
C	–5.27665603	2.05950084	3.56491556
C	–6.65909633	2.11239772	3.68925123
C	–7.44857047	1.24858126	2.94110298
C	–6.85000369	0.33799625	2.08075873
C	5.00322655	0.37041665	2.54166637
C	5.68993789	–0.57842426	1.78226382
C	7.06688979	–0.73164270	1.85921722
C	7.79742899	0.06041277	2.73494089
C	7.14402526	1.00080884	3.52097881
C	5.76628763	1.14322965	3.41980982
C	0.82780418	9.22590027	–1.65734826
C	1.44181538	11.49866443	–1.44242292
C	0.52539637	5.37313778	0.22594278
C	0.14031446	5.56604776	–1.10821255
C	0.24420446	6.81783697	–1.70048910
C	0.73446708	7.90585084	–0.97151155
C	1.11783595	7.72297877	0.36136640
C	1.01283002	6.46851320	0.95143255
C	–1.44021347	–11.49967642	1.44011290
C	–0.82646652	–9.22683553	1.65564511
N	–1.35489915	0.48424637	–2.70238720
N	1.09877551	0.04469128	–3.02236613
N	1.16200747	–2.26670941	–1.59759386
N	–1.66619614	–2.09326609	–1.80224104
N	–1.16196514	2.26677639	1.59720658
N	–1.09921070	–0.04448129	3.02226379
N	1.35443951	–0.48446039	2.70258294
N	1.66621938	2.09292510	1.80213963
O	0.92358526	0.72502229	–0.41000743

O	–0.92377402	–0.72518895	0.40998350
O	0.50390449	9.42287544	–2.80777093
O	1.31771087	10.18926581	–0.85429860
O	–1.31624779	–10.19008979	0.85237517
O	–0.50250229	–9.42398517	2.80601580
F	5.17338023	2.05720416	4.20040350
F	7.84414200	1.75798904	4.37289480
F	9.12141353	–0.08093922	2.82113353
F	7.69306100	–1.62917567	1.08827665
F	5.02150751	–1.36744031	0.92733602
F	–4.54729177	2.91177407	4.29879384
F	–7.23426390	2.98638851	4.52278119
F	–8.77789066	1.29513095	3.04859626
F	–7.60801084	–0.48644589	1.34653479
F	–4.92581626	–0.60077946	1.14474166
F	–5.02171587	1.36690138	–0.92679647
F	–7.69330421	1.62835355	–1.08721678
F	–9.12185063	0.07991923	–2.81975769
F	–7.84467859	–1.75892438	–4.37171252
F	–5.17388019	–2.05788239	–4.19972047
F	4.54790398	–2.90980830	–4.29973890
F	7.23497358	–2.98357773	–4.52321130
F	8.77783054	–1.29284120	–3.04762717
F	7.60712838	0.48737765	–1.34471332
F	4.92482183	0.60093152	–1.14351810
H	–4.86484619	–2.87161243	–1.38775576
H	–3.19230922	–4.77362288	–0.58577959
H	2.24875576	–5.19973413	–0.53322430
H	4.18347254	–3.59765530	–1.40911174
H	3.89751269	1.18084939	–4.32349737
H	1.74106256	2.63358062	–4.95944195
H	–1.60158473	2.85977346	–4.96748507
H	–3.95111022	1.85598334	–4.17037567
H	–1.30042068	–6.33590281	–1.98861436
H	–1.74199299	–2.63282123	4.95990577
H	–3.89814509	–1.17977158	4.32371003
H	–4.18314987	3.59830549	1.40842229
H	–2.24811822	5.19980093	0.53223350
H	3.19285717	4.77286122	0.58541567
H	4.86503394	2.87076148	1.38799735
H	3.95028687	–1.85619089	4.17123400
H	1.60050990	–2.85955015	4.96821099
H	0.46547535	11.86791283	–1.75863487
H	1.85414359	12.13011936	–0.65933036
H	2.11134581	11.46740196	–2.30277114
H	–0.22846579	4.72455742	–1.68270315

H	–0.04621090	6.96865195	–2.73263664
H	1.49088612	8.56293494	0.93186389
H	1.30099899	6.33573411	1.98761559
H	–1.85208338	–12.13105828	0.65671794
H	–2.11009702	–11.46880126	2.30020109
H	–0.46388735	–11.86871554	1.75659447
H	–1.48990684	–8.56337781	–0.93334915
H	0.04736914	–6.96972613	2.73135022
H	0.22923772	–4.72537497	1.68190725
Sb	–0.13962147	–0.65384077	–1.44549241
Sb	0.13942486	0.65370409	1.44547036

Table S4. TD–DFT Calculations of Singlets for **2** Monomer

State	Energy	Wavelength	Oscillator Strength	Orbital Contributions[a]
S_1	2.2911	541.16	0.1624	23% HOMO–1 → LUMO+1, 77% HOMO → LUMO
S_2	2.3596	525.45	0.0338	34% HOMO → LUMO+1, 66% HOMO–1 → LUMO
S_3	3.0684	404.06	1.2911	33% HOMO–1 → LUMO, 67% HOMO → LUMO+1
S_4	3.1019	399.70	1.1879	23% HOMO → LUMO, 77% HOMO–1 → LUMO+1
S_5	3.2798	378.02	0.0086	13% HOMO → LUMO+2, 87% HOMO → LUMO+3
S_6	3.3991	364.75	0.0024	12% HOMO–1 → LUMO+2, 88% HOMO–1 → LUMO+3
S_7	3.5366	350.57	0.0012	14% HOMO → LUMO+3, 86% HOMO → LUMO+2
S_8	3.6133	343.14	0.0177	21% HOMO–3 → LUMO, 79% HOMO–2 → LUMO
S_9	3.6164	342.83	0.0080	19% HOMO–2 → LUMO, 81% HOMO–3 → LUMO
S_{10}	3.7048	334.65	0.0233	12% HOMO–1 → LUMO+3, 88% HOMO–1 → LUMO+2
S_{11}	3.7648	329.33	0.0005	18% HOMO–4 → LUMO, 35% HOMO–8 → LUMO, 36% HOMO–5 → LUMO
S_{12}	3.8932	318.46	0.0078	33% HOMO–5 → LUMO, 67% HOMO–4 → LUMO
S_{13}	3.9132	316.83	0.0033	100% HOMO → LUMO+4
S_{14}	3.9243	315.94	0.0061	100% HOMO → LUMO+5
S_{15}	3.9378	314.86	0.0019	84% HOMO–7 → LUMO

[a] Calculated from the normalized coefficients of the excitation wavefunction: % = (x_i^2 / Σ x_i^2) × 100; transition contributions of < 10% have been excluded.

Table S5. TD–DFT Calculations of Triplets for **2** Monomer

State	Energy	Wavelength	Orbital Contributions[a]
T_1	1.5267	812.12	95% HOMO → LUMO
T_2	1.6644	744.94	21% HOMO → LUMO+1, 79% HOMO–1 → LUMO
T_3	1.9901	623.00	22% HOMO–1 → LUMO, 78% HOMO → LUMO+1
T_4	2.2411	553.23	97% HOMO–1 → LUMO+1
T_5	3.0941	400.72	13% HOMO → LUMO+2, 87% HOMO → LUMO+3
T_6	3.2383	382.87	17% HOMO–5 → LUMO, 32% HOMO–8 → LUMO, 35% HOMO–2 → LUMO
T_7	3.3251	372.87	13% HOMO–5 → LUMO+2, 18% HOMO–4 → LUMO+2, 51% HOMO → LUMO+2
T_8	3.3284	372.50	10% HOMO–1 → LUMO+2, 78% HOMO–1 → LUMO+3
T_9	3.3909	365.64	11% HOMO–11 → LUMO, 11% HOMO–1 → LUMO+3, 67% HOMO–3 → LUMO
T_{10}	3.4631	358.01	10% HOMO–5 → LUMO, 14% HOMO–8 → LUMO, 53% HOMO–2 → LUMO
T_{11}	3.5911	345.26	17% HOMO–2 → LUMO+1, 29% HOMO–11 → LUMO
T_{12}	3.6379	340.82	11% HOMO–5 → LUMO+2, 14% HOMO–4 → LUMO+2, 47% HOMO → LUMO+2
T_{13}	3.6450	340.15	76% HOMO–3 → LUMO+3
T_{14}	3.6548	339.24	10% HOMO–1 → LUMO+3, 24% HOMO–2 → LUMO+3, 32% HOMO–1 → LUMO+2
T_{15}	3.6639	338.39	35% HOMO–2 → LUMO+3, 37% HOMO–1 → LUMO+2

[a] Calculated from the normalized coefficients of the excitation wavefunction: % = (x_i^2 / Σ x_i^2) × 100; transition contributions of <10% have been excluded.

References

(1) C. M. Lemon, S. J. Hwang, A. G. Maher, D. C. Powers and D. G. Nocera, *Inorg. Chem.*, 2018, **57**, 5333–5342.

(2) G. R. Fulmer, A. J. M. Miller, N. H. Sherden, H. E. Gottlieb, A. Nudelman, B. M. Stoltz, J. E. Bercaw and K. I. Goldberg, *Organometallics*, 2010, **29**, 2176–2179.

(3) *CRC Handbook of Chemistry and Physics*, 84th ed., CRC Press, Boca Raton, 2003.

(4) R. Sens and K. H. Drexhage, *J. Lumin.*, 1981, **24/25**, 709–712.

(5) C. M. Lemon, E. Karnas, M. G Bawendi and D. G. Nocera, *Inorg. Chem.*, 2013, **52**, 10394–10406.

(6) Z. H. Loh, S. E. Miller, C. J. Chang, S. D. Carpenter and D. G. Nocera, *J. Phys. Chem. A*, 2002, **106**, 11700–11708.

(7) A. A. Pizano, D. A. Lutterman, P. G. Holder, T. S. Teets, J. Stubbe and D. G. Nocera, *Proc. Natl. Acad. Sci. U.S.A.*, 2012, **109**, 39–43.

(8) P. G. Holder, A. A. Pizano, B. L. Anderson, J. Stubbe and D. G. Nocera, *J. Am. Chem. Soc.*, 2012, **134**, 1172–1180.

(9) A. D. Becke, *Phys. Rev. A*, 1988, **38**, 3098–3100.

(10) A. D. Becke, *J. Chem. Phys.*, 1993, **98**, 1372–1377.

(11) A. D. Becke, *J. Chem. Phys.*, 1993, **98**, 5648–5652.

(12) C. Lee, W. Yang and R. G. Parr, *Phys. Rev. B*, 1988, **37**, 785–789.

(13) M. J. Frisch, G. W. Trucks, H. B. Schlegel, G. E. Scuseria, M. A. Robb, J. R. Cheeseman, G. Scalmani, V. Barone, B. Mennucci, G. A. Petersson, H. Nakatsuji, M. Caricato, X. Li, H. P. Hratchian, A. F. Izmaylov, J. Bloino, G. Zheng, J. L. Sonnenberg, M. Hada, M. Ehara, K. Toyota, R. Fukuda, J. Hasegawa, M. Ishida, T. Nakajima, Y. Honda, O. Kitao, H. Nakai, T. Vreven, J. A. Montgomery, Jr., J. E. Peralta, F. Ogliaro, M. Bearpark, J. J. Heyd, E. Brothers, K. N. Kudin, V. N. Staroverov, R. Kobayashi, J. Normand, K. Raghavachari, A. Rendell, J. C. Burant, S. S. Iyengar, J. Tomasi, M. Cossi, N. Rega, J. M. Millam, M. Klene, J. E. Knox, J. B. Cross, V. Bakken, C. Adamo, J. Jaramillo, R. Gomperts, R. E. Stratmann, O. Yazyev, A. J. Austin, R. Cammi, C. Pomelli, J. W. Ochterski, R. L. Martin, K. Morokuma, V. G. Zakrzewski, G. A. Voth, P. Salvador, J. J. Dannenberg, S. Dapprich, A. D. Daniels, Ö. Farkas, J. B. Foresman, J. V. Ortiz, J. Cioslowski, and D. J. Fox, *Gaussian 09*, Revision D.01; Gaussian, Inc., Wallingford, CT, 2009.

(14) J. H. Wood and A. M. Boring, *Phys. Rev. B*, 1978, **18**, 2701–2711.

(15) V. Barone and M. Cossi, *J. Phys. Chem. A*, 1998, **102**, 1995–2001.

(16) M. Cossi, N. Rega, G. Scalmani and V. Barone, *J. Comput. Chem.*, 2003, **24**, 669–681.

(17) R. Bauernschmitt and R. Ahlrichs, *Chem. Phys. Lett.*, 1996, **256**, 454–464.

(18) M. E. Casida, C. Jamorski, K. C. Casid and D. R. Salahub, *J. Chem. Phys.*, 1998, **108**, 4439–4449.

(19) R. E. Stratmann, G. E. Scuseria and M. J. Frisch, *J. Chem. Phys.*, 1998, **109**, 8218–8224.

(20) C. Van Caillie and R. D. Amos, *Chem. Phys. Lett.*, 1999, **308**, 249–255.

(21) G. Scalmani, M. J. Frisch, B. Mennucci, J. Tomasi, R. Cammi and V. Barone, *J. Chem. Phys.*, 2006, **124**, 094107/1–15.

(22) M. D. Hanwell, D. E. Curtis, D. C. Lonie, T. Vandermeersc, E. Zurek and G. R. Hutchison, *J. Cheminform.*, 2012, **4**, 17/1–17.

(23) Bruker Analytical X-ray Systems, Inc. *SAINT and APEX 2 Software for CCD Diffractometers*, Bruker Analytical X-ray Systems, Inc., Madison, WI, USA, 2000.

(24) G. M. Sheldrick, *SADABS*, Bruker Analytical X-ray Systems, Inc., Madison, WI, USA, 2014.

(25) G. M. Sheldrick, *SHELXT*, University of Göttingen, Germany, 2014.

(26) G. M. Sheldrick, *Acta Crystallogr. Sect. A: Found. Crystallogr.*, 2015, **A71**, 3–8.

(27) G. M. Sheldrick, *SHELXL*, University of Göttingen, Germany, 2014.

(28) G. M. Sheldrick, *Acta Crystallogr. Sect. C: Cryst. Struct. Commun.*, 2015, **C71**, 3–8.

(29) O. V. Dolomanov, L. J. Bourhis, R. J. Gildea, J. A. K. Howard and H. Puschmann, *J. Appl. Crystallogr.*, 2009, **42**, 339–341.

(30) A. L. Spek, *Acta Crystallogr. Sect. C: Cryst. Struct. Commun.*, 2015, **C71**, 9–18.